

AD-768 352

ELEMENTAL ANALYSIS OF MATERIALS BY ENERGY-  
DISPERSIVE SPECTROMETRY OF X-RAYS  
PRODUCED BY A FOCUSING ELECTRON GUN

William Charles Nielsen, Jr.

Air Force Institute of Technology  
Wright-Patterson Air Force Base, Ohio

March 1973

DISTRIBUTED BY:

**NTIS**

National Technical Information Service  
U. S. DEPARTMENT OF COMMERCE  
5285 Port Royal Road, Springfield Va. 22151

ELEMENTAL ANALYSIS OF MATERIALS BY  
ENERGY-DISPERSIVE SPECTROMETRY OF X RAYS  
PRODUCED BY A FOCUSING ELECTRON GUN  
THESIS

GEP/PH/73-16

William C. Nielsen, Jr.  
Captain USAF

Approved for public release; distribution unlimited.

iv

Unclassified

Security Classification

AU-768352

## DOCUMENT CONTROL DATA - R &amp; D

(Security classification of title, body of abstract and indexing annotation must be entered when the overall report is classified)

1. ORIGINATING ACTIVITY (Corporate author)

Air Force Institute of Technology (AFIT-EN)  
Wright-Patterson AFB, Ohio 45433

2a. REPORT SECURITY CLASSIFICATION

Unclassified

2b. GROUP

3. REPORT TITLE

Elemental Analysis of Materials by Energy Dispersive Spectrometry of  
X rays Produced by a Focusing Electron Gun

4. DESCRIPTIVE NOTES (Type of report and inclusive dates)

AFIT Thesis

5. AUTHOR(S) (First name, middle initial, last name)

William C. Nielsen, Jr.  
Captain USAF

6. REPORT DATE

March 1973

7a. TOTAL NO. OF PAGES

88 98

7b. NO. OF REFS

31

8a. CONTRACT OR GRANT NO.

b. PROJECT NO.

c.

d.

9a. ORIGINATOR'S REPORT NUMBER(S)

GEP/PH/73-16 ✓

9b. OTHER REPORT NO(S) (Any other numbers that may be assigned  
this report)

10. DISTRIBUTION STATEMENT

Approved for public release, distribution unlimited.

11. SUPPLEMENTARY NOTES

Approved for public release; IAW AFR 190-17

JERRY C. HIX, Captain, USAF  
Director of Information

12. SPONSORING MILITARY ACTIVITY

Air Force Institute of Technology  
Wright-Patterson AFB, Ohio 45433

13. ABSTRACT

The construction and operation of a system for elemental analysis of materials by energy-dispersive x-ray analysis are described. The majority of the components are found in most well-equipped physics laboratories while others such as the electron gun are relatively inexpensive to fabricate. The Steigerwalt electron gun provides a beam of electrons which can be varied in diameter from a fraction of a millimeter to several centimeters. Fluorescent x rays from samples are excited either directly by electrons from the gun or by secondary x rays produced by using the electrons to excite interchangeable thin targets. With electron energies up to 40 keV and beam currents as high as 300  $\mu$ A, elemental concentrations as low as  $10^{-7}$  g and less than 10 ppm have been detected with short exposures. The sensitivity of this system is compared to systems which use radionuclides and protons to excite x rays. All x-ray measurements were made with an intrinsic germanium detector with a resolution (FWHM) of 200 eV at 6.4 keV.

Reproduced by

NATIONAL TECHNICAL  
INFORMATION SERVICEU S Department of Commerce  
Springfield VA 22151DD FORM 1473  
1 NOV 65

Unclassified

Security Classification

Unclassified

Security Classification

KEY WORDS

LINK A

LINK B

LINK C

ROLE

WT

ROLE

WT

ROLE

WT

Energy Dispersive X-ray Analysis

Electron Gun

Fluorescent X rays

Elemental Analysis

Trace Analysis

Unclassified

Security Classification

1a

ELEMENTAL ANALYSIS OF MATERIALS BY  
ENERGY-DISPERSIVE SPECTROMETRY OF X RAYS  
PRODUCED BY A FOCUSING ELECTRON GUN

THESIS

Presented to the Faculty of the School of Engineering  
of the Air Force Institute of Technology

Air University

In Partial Fulfillment of the  
Requirements for the Degree of  
Master of Science

by

William C. Nielsen Jr., B.S.B.S.

Captain

USAF

Graduate Engineering Physics

March 1973

Approved for public release; distribution unlimited.

10

### Preface

The field of energy dispersive x-ray spectrometry is progressing so rapidly, that with the resources of some large scientific companies and laboratories devoted almost exclusively to its development, it is difficult to keep up with the innovations financially or make any contributions technologically. However, I think our efforts here to develop systems with comparable results at lower costs have been reasonably successful, and the absence of complete automation is a more desirable situation in academic applications.

I would like to thank Dr. G. John and Dr. G. R. Hagee for the opportunity to do this study, and for their advice and help in completing it. I would also like to acknowledge the valuable assistance I received from J. Miskimen, G. Gergal, R. Hendricks, and R. Gabriel of the Physics Department and M. Wolfe of the AFIT Shop.

My thanks and acknowledgment also to Dr. R. L. Hengehold for his advice and the design for the electron gun which I used to obtain all the data presented in this paper.

Finally, I would like to thank my family for their patience while my time and energy were devoted to this project.

W. C. Nielsen, Jr.

Contents

	Page
Preface. . . . .	ii
List of Figures. . . . .	v
List of Tables . . . . .	vi
Abstract . . . . .	vii
I. Introduction . . . . .	1
II. Theory . . . . .	5
Production of X rays. . . . .	5
Fluorescent Yield . . . . .	8
Absorption of X rays. . . . .	9
Scattering of X rays. . . . .	9
Coherent Scatter . . . . .	10
Compton or Incoherent Scatter. . . . .	11
X-ray Spectra . . . . .	11
Characteristic X rays. . . . .	11
Background . . . . .	12
Sources of Excitation . . . . .	14
Radioisotopes. . . . .	16
Electrons. . . . .	16
Protons. . . . .	18
X-ray Tubes and Electron Guns. . . . .	18
Electron Range. . . . .	21
Matrix Effects. . . . .	22
III. Equipment. . . . .	25
Detector-Analyzer System. . . . .	25
Detector . . . . .	25
Multichannel Analyzer. . . . .	27
Scattering Chamber. . . . .	27
Electron Gun. . . . .	30
IV. Experimental Procedure . . . . .	36
Equipment Calibration and Operation . . . . .	36
Transmission X-ray Excitation . . . . .	39
Target Selection . . . . .	39
Sample Preparation . . . . .	43
Trace Analysis . . . . .	45
Analysis of Solids . . . . .	49
Direct Electron Excitation. . . . .	50

	Page
V. Data Analysis and Results. . . . .	54
System Operation. . . . .	54
Trace Element Analysis. . . . .	59
Matrix Effects. . . . .	66
VI. Conclusions and Recommendations. . . . .	74
Appendix A: List of Equipment . . . . .	78
Appendix B: Statistical Treatment . . . . .	80
Appendix C: Proposed Sample Chamber . . . . .	83
Bibliography . . . . .	85
Vita . . . . .	88



List of Figures

Figure		Page
1	Partial Energy Level Diagram. . . . .	7
2	Variation of Fluorescent Yield with Energy for K and L X rays. . . . .	8
3	Mass Absorption Coefficient vs. Energy for Mo .	10
4	Typical Energy Spectrum . . . . .	15
5	Total X-ray Yields for Excitation by Electrons Protons, and Primary X rays . . . . .	17
6	X-ray Transmission Through Balanced Filters of Copper and Nickel. . . . .	20
7	Detector-Analyzer System. . . . .	26
8	Arrangement of Scattering Chamber, Detector, and Electron Gun. . . . .	29
9	Effect of Filament Position on Electron Beam Characteristics . . . . .	31
10	Electron Gun. . . . .	33
11	Circuit Diagram for the Electron Gun. . . . .	35
12	Optimum Geometry for Transmission Foil Excitation. . . . .	40
13	Carousel Sample Holder. . . . .	47
14	Chamber Set-up for Excitation of Steel Using Iron Secondary Target . . . . .	51
15	Intensity as a Function of Electron Beam Current . . . . .	55
16	Intensity as a Function of Electron Beam Potential . . . . .	57
17	Concentration vs. Intensity for Cr and Fe . . .	61
18	Concentration vs. Intensity for Rb and La . . .	62
19	Spectrum From Atmospheric Dust Excited with a Mo Target . . . . .	67
20	Proposed Sample Chamber . . . . .	84

List of Tables

Table		Page
I	Variation of Electron Beam Diameter With Other System Parameters. . . . .	59
II	Contaminants in Atmospheric Dust (5.5 mg). . . . .	68
III	Enhancement of Chromium in Steel From an Iron Target Used as Both a Primary and Secondary Exciting Source. . . . .	69
IV	Composition of Steel Estimated by Direct Electron Excitation. . . . .	73
V	Net Peak Areas From the Excitation of $10^{-5}$ g of Chromium. . . . .	81

Abstract

The construction and operation of a system for elemental analysis of materials by energy-dispersive x-ray analysis are described. The majority of the components are found in most well-equipped physics laboratories while others such as the electron gun are relatively inexpensive to fabricate. The Steigerwalt electron gun provides a beam of electrons which can be varied in diameter from a fraction of a millimeter to several centimeters. Fluorescent x rays from samples are excited either directly by electrons from the gun or by secondary x rays produced by using the electrons to excite interchangeable thin targets. With electron energies up to 40 keV and beam currents as high as 300  $\mu$ A elemental concentrations as low as  $10^{-7}$  g and less than 10 ppm have been detected with short exposures. The sensitivity of this system is compared to systems which use radionuclides and protons to excite x rays. All x-ray measurements were made with an intrinsic germanium detector with a resolution (FWHM) of 200 eV at 6.4 keV.

# ELEMENTAL ANALYSIS OF MATERIALS BY ENERGY-DISPERSIVE SPECTROMETRY OF X RAYS PRODUCED BY A FOCUSING ELECTRON GUN

## I. INTRODUCTION

The purpose of this thesis was to design, construct, and investigate the capabilities of a system for qualitative and quantitative energy dispersive x-ray spectrometry using an electron gun and scattering chamber. This was to provide an additional method of excitation to complement radioisotope and proton excitation systems also being developed.

The use of energy dispersive spectrometry became practical only recently (1966), with the development of detectors with resolution good enough to separate the energies of adjacent elements. Prior to this, the method of wavelength dispersion or diffraction was the only one in general use. This method relies on the Bragg equation relating a photon's wavelength to its angle of diffraction from an analyzing crystal. It is a very accurate technique but has some disadvantages when compared to energy dispersion. One disadvantage is that only one wavelength at a time can be examined. The geometrical alignment of the system must also be very precise and the system components are complex, non-moveable, and require a large amount of space (Ref 23:6). In addition, the complexity of line spectra compared to energy spectra makes identification of elements in the specimen more difficult. By contrast, the complete energy spectrum of a specimen is generated simultaneously, geometry is not as critical, and the

system is less complex.

The development of solid state detectors with silicon or germanium crystals of high resolution provided the breakthrough necessary to make energy dispersion an accurate technique. Detectors with resolution as low as 100 eV (FWHM) are now available as well as some very sophisticated equipment to display and analyze energy spectra. Electron microprobes and microscopes used as exciting sources can not only excite characteristic x rays in a specimen but also provide images of the surfaces excited. Systems using these sources plus radioisotope and x-ray tube excitation are available commercially which excite the specimen, detect and display the characteristic spectrum, automatically strip the background, integrate the peak areas, and provide a qualitative and quantitative readout of the elements present within minutes (Ref 24,18).

Unfortunately, these advanced systems are very expensive and their cost may be prohibitive for many university physics departments. The aim of this project was to build an inexpensive system using components generally available in a college physics laboratory. The only component that was not in the inventory at the beginning of the project was the electron gun which was subsequently fabricated in the school machine shop at a cost of approximately two hundred dollars. The Ortec scattering chamber used in the system is an expensive piece of equipment, but can be replaced by a simpler and more suitable design. This is recommended because of the

geometrical limitations encountered in this study using the large Ortec chamber.

Analysis of simple spectral data can be done by hand or analyzed with the aid of a computer program developed for use with the CDC 6600 computer. The program provides peak identification or rejection, and computation of peak areas, relative intensities and relative detector efficiencies (Ref 3.1).

An electron gun was used primarily to produce characteristic x rays in thin transmission foils which in turn excited characteristic x rays in samples placed in the scattering chamber. Selective excitation was possible using different foils and the limit of detectability was kept constant throughout the range of elements examined. Concentrations as low as 0.1  $\mu\text{g}$  were detected and graphs relating concentration and intensity were plotted for several elements up to 0.01 g using the technique of evaporating known concentrations of metal salts on a mylar backing.

The use of a finely focused beam of electrons showed promise as an analytical tool for determining the composition and concentration of elements in thick specimens. Attempts to correlate intensity and weight concentration by direct electron excitation of National Bureau of Standards steels with minimal matrix effects and mathematical unfolding gave reasonably good results.

The intrinsic germanium detector used during the experiments gave consistent 200 eV (FWHM) resolution and was able to detect and resolve elements as low as aluminum, although the efficiency drops off rapidly below chlorine. The

detector will efficiently measure photon energies up to 100 keV which includes the K x rays of all elements through americium. The escape peaks inherent with the use of germanium detectors can be minimized by the selective use of target foils. The use of a silicon detector will increase the efficiency of detection of elements below  $Z=30$ , and allow the investigation of elements as low as oxygen, but does not compare in total energy range to germanium.

This report is organized into six main sections. Section II deals briefly with the theory of x-ray production and analysis, and Section III describes the equipment used in the experiments. Section IV is a description of the experimental set-up and procedure, while Section V is devoted to the analysis of the data and discussion of the results. The conclusions and recommendations are presented in Section VI, and statistics and auxiliary data in the Appendices.

## II. THEORY

The theory of x-ray production and interaction, and the interpretation of energy dispersive x-ray spectra are discussed in this section. The energy spectrum is the end product of a series of processes which must be understood to obtain accurate data and analyze results. Such factors as fluorescent yield and cross section which govern photon interactions and x-ray intensity must be covered plus the differences between charged particle and photon generation of x rays.

Both particles and photons also undergo interactions which do not contribute to the characteristic spectrum. These interactions combined with imperfections in the detection system produce background which can obscure desired data.

The interactions which can occur between characteristic x rays in the specimen matrix must also be known and eliminated if quantitative analysis is to be accomplished.

All of the processes or phenomena which affect the use of energy dispersive spectrometry are considered briefly in the following discussion.

### Production of X rays

X rays are produced in a two-step process in which a quantum of energy, either a photon or a charged particle, must first interact with an atom to eject an inner shell electron. The atom then de-excites by the emission of an



x ray or Auger electron. The electron cannot be removed unless the incident quantum has an energy greater than the energy which binds the electron to the nucleus. When the vacancy is filled by an outer shell electron, that electron must give up energy to occupy a more tightly bound shell and the x ray emitted during the transition is exactly equal to the energy difference between the two shells. Binding energies increase with atomic number because of the change in the attractive force between the nucleus and orbital electrons. Thus the energies of x rays emitted in transitions between electron shells are characteristic of particular elements.

The intensities of transition between various electron shells in an atom depend on the probability of their occurrence which may be calculated from the principles of quantum mechanics. Fig. 1 is a partial energy level diagram showing some of the possible transitions. According to the dipole selection rules, the orbital quantum number must change by  $\pm 1$  and the total angular momentum must change by  $\pm 1$  or 0 for an allowed radiative transition. Generally the most probable and therefore most intense transitions in a series are those which involve the least total energy change. The  $K_{\alpha}$  intensity is always greater than the  $K_{\beta}$ , and the  $L_{\alpha}$  and  $L_{\beta}$  are similar to each other and greater than the other L transitions.

The difference in energy between the ground state and each shell is called the binding energy and gives the location of the absorption edge. It is larger than any fluorescent transition since it represents the minimum energy

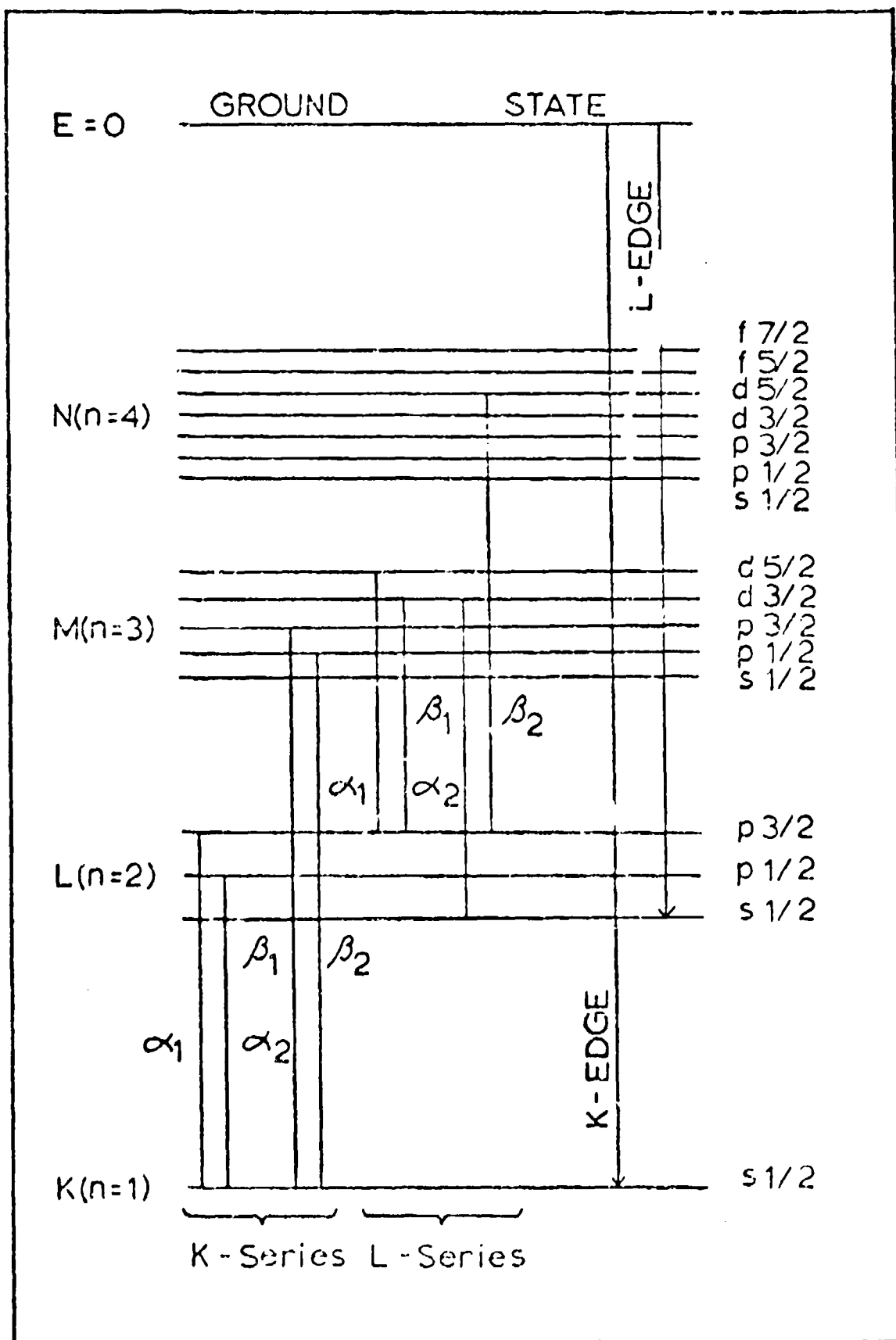


Fig. 1. Partial Energy Level Diagram

necessary to eject an electron from its shell.

### Fluorescent Yield

When an atom does not de-excite by x ray emission, a competing mode called the Auger effect occurs which results in the ejection of an electron from another shell. This creates additional vacancies which may lead to further x-ray or Auger emission. The K-shell fluorescent yield is defined as the probability that a K x ray will be emitted when a K-shell vacancy is created. The probability of Auger emission is high for the K-shells of the light elements and the L-shells of many elements. The fluorescent yield for these elements therefore is low as shown in Fig. 2, and they are difficult to detect because of their low x-ray intensity (Ref 11:183).

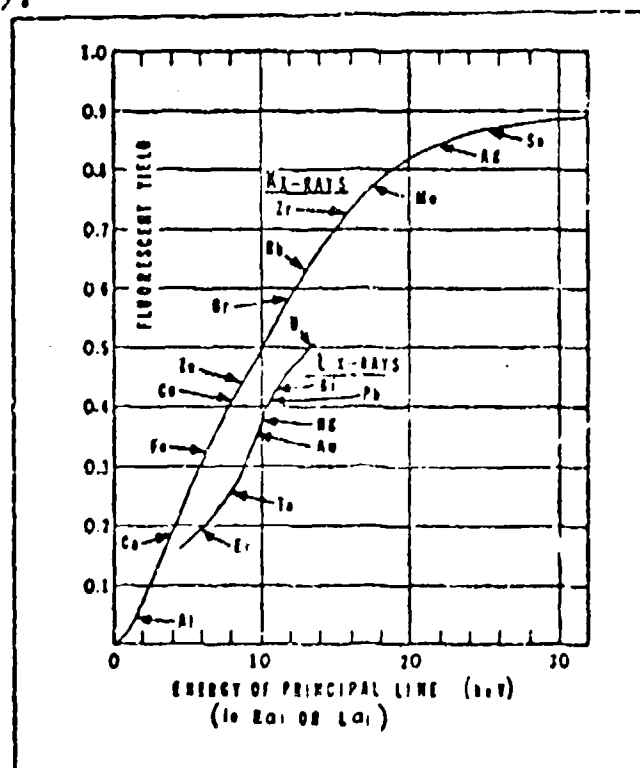


Fig. 2. Variation of Fluorescent Yield with Energy for K and L X rays (Ref 7:6)

Absorption of X rays

X rays are absorbed in the same way as all electromagnetic radiation. The loss of intensity,  $dI$ , when passing through an incremental thickness,  $dx$ , is proportional to the intensity,  $I$ . The constant of proportionality is called the linear absorption coefficient,  $\mu$ , which is the interaction probability per unit path length for absorption interactions and is a function of the energy of the incident radiation. This relationship is written

$$dI = -\mu I dx \quad (1)$$

which after integration becomes

$$I = I_0 e^{-\mu x} \quad (2)$$

where  $I_0$  is the intensity of the incident photons and  $I$  is the intensity transmitted through a slab of thickness,  $x$ . Since photoelectric absorption is most probable when the energy of the incident radiation is just above the absorption edge, the value of  $\mu$  increases abruptly just as the edge is exceeded. This can be seen in Fig. 3 which shows the relationship between the absorption coefficient and the exciting energy for molybdenum. Eq (2) is a relatively simple relationship, but very useful when determining transmission or filtering of x rays through target foils.

Scattering of X rays

The radiation that is not photoelectrically absorbed can interact with atoms in other ways. If the energy of the

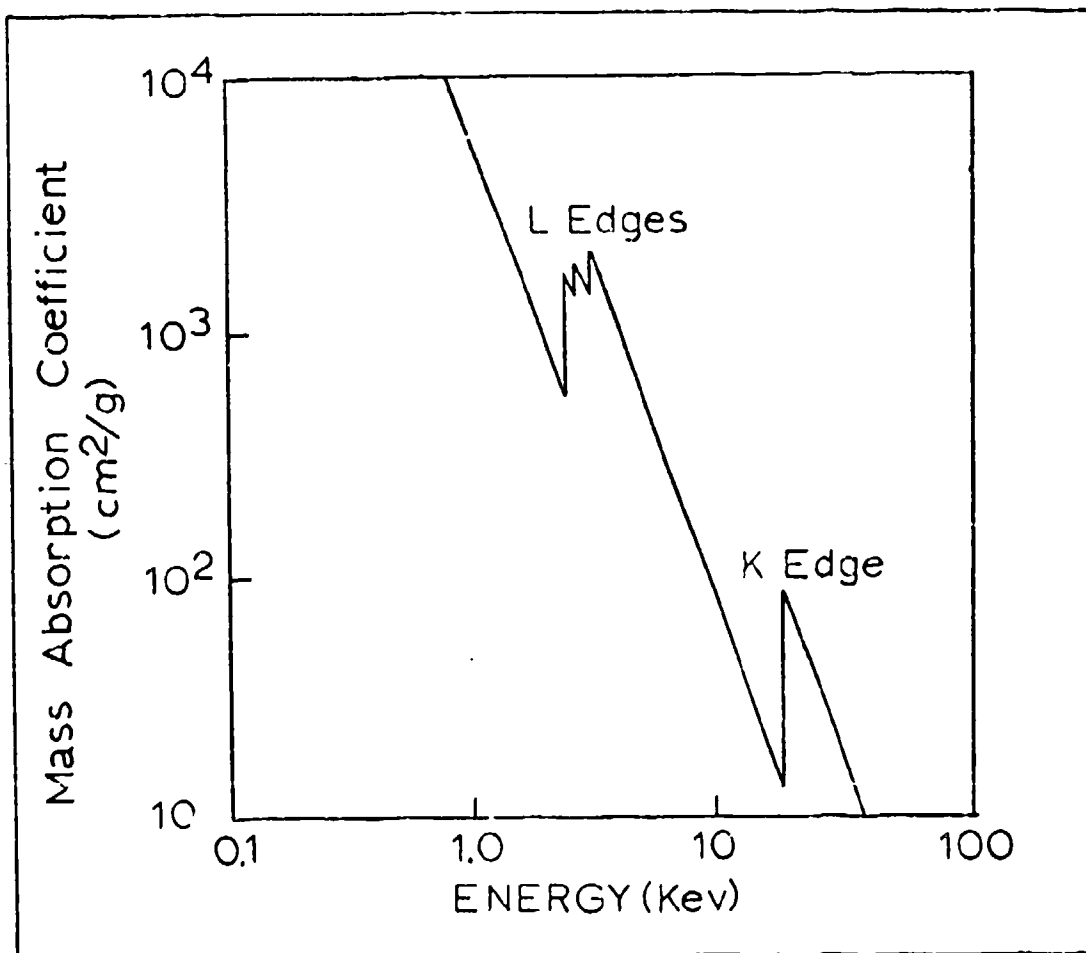


Fig. 3. Mass Absorption Coefficient vs. Energy for Mo (Ref 1:11)

incident radiation is greater than 1.02 MeV, pair production can occur resulting in the creation of an electron-positron pair. This mechanism is not usually observed in fluorescent x-ray production because of the low energies ( $E < 100$  keV) involved. Most of the non-absorption interaction consists of scattering collisions with atoms and electrons.

Coherent Scatter. Coherent or Rayleigh scatter occurs when a photon collides with an atom and changes direction, but retains almost all of its original energy. Because of

the massive size of the atom compared to the photon, almost no energy is transferred. Rayleigh scattered photons are not distributed isotropically.

Compton or Incoherent Scatter. Photons can also interact with orbital electrons, and during these collisions some of the energy of the photon is transferred to the electron. The total amount is a function of the scattering angle and can be computed from the following equation:

$$E' = \frac{E}{1 + \frac{E}{M_0 C^2} (1 - \cos \theta)} \quad (3)$$

where

$E'$  = energy of the scattered photon

$E$  = energy of the incident photon

$\theta$  = angle between the directions of the incident and scattered photons

$M_0 C^2$  = rest energy of the electron

### X-ray Spectra

Characteristic X ray. Since each x ray is characteristic of a particular element, the element can be identified in a compound or mixture by exciting the atoms in the substance and measuring the energies of the emitted x rays. A typical x-ray spectrum consists of peaks characteristic of K and L-shell x rays from the sample plus a continuum of background caused by scattering, electronic noise, stray environmental radiation and bremsstrahlung if electrons or protons are the exciting source.

Interpreting the characteristic spectrum is not always

a simple process because of interferences. The  $K_{\beta}$  x rays of some elements are very close in energy to the  $K_{\alpha}$  x rays of others, and may overlap in the spectrum because of the limitations of detector resolution. If a  $K_{\beta}$  peak is hidden under the  $K_{\alpha}$  peak of another element, its presence will probably be suspected only if accompanied by its own  $K_{\alpha}$  peak. Then the combination peak can be reduced to its component parts by comparing the  $K_{\alpha}$  and  $K_{\beta}$  relative intensities of the two interfering elements. Interferences can also occur between the K and L x-ray peaks of different elements and are harder to detect.

Background. The most obvious background is caused by scattering interactions in both the sample and the detector.

The low end of the energy spectrum is dominated by Compton scattering of photons in the detector material. After colliding with an electron, the scattered photon escapes from the detector, depositing only the energy that it transferred to the electron.

The exciting radiation is scattered both coherently and incoherently in the sample. The Compton scatter appears in the spectrum as a large broad peak lower in energy than the radiation from the exciting source. Its exact position depends on the experimental geometry and can be calculated from Eq (3). The coherent peak is generally less intense than the Compton peak and appears at an energy corresponding to that of the exciting radiation.

Another source of background involves the production of photoelectrons in the detector material. If the characteristic x rays produced by photoelectric interaction escape

without being absorbed in the detector, the total energy deposited is equal to the energy of the incident photon minus the K- or L-shell energy characteristic of the detector material. The resulting spectrum peaks are called escape peaks. Large scatter peaks will generally be the source of corresponding escape peaks. Silicon detectors are less affected by this mechanism than germanium because silicon x rays are lower in energy and are less likely to escape. The photoelectrons can also escape from the detector surface without depositing their total energy resulting in a continuous background that is typically less than 1% of the counts in the scatter peaks for silicon detectors (Ref 7:24).

A certain amount of noise is inherent in the electronics associated with the detector and preamp. The input field-effect transistor (FET) in the preamp can be a major source of noise which degrades the resolution of the detector. Most recent improvements have been aimed at reducing this noise. Cooling of the FET combined with the development of a pulsed optical feedback system have been the most significant improvements. The optical system replaces resistive feedback which can add 60 eV or more to the energy resolution (Ref 28:115).

One of the largest sources of continuous background has been identified as charge loss or poor charge collection in the detector. Tailing on the low energy side of spectral peaks and a non-gaussian peak shape are indications of charge loss. To alleviate this problem, new detectors are being



designed with improved geometry that result in better definition of the sensitive volume (Ref 7:25).

When charged particles are used as the source of excitation, continuous bremsstrahlung radiation is emitted as the particles are decelerated in collisions with atoms and can constitute a large fraction of the total background. Electrons may lose all or only a part of their energy in a single collision, and therefore a range of bremsstrahlung energies from zero up to the energy of the electron beam is observed. The maximum intensity occurs at an energy equal to two-thirds of the beam voltage (Ref 28:119). The peak to background ratio of electron-excited spectra increases as beam voltage increases because of the greater efficiency of production of characteristic x rays at higher electron energies.

Protons also emit continuous radiation when they are decelerated, but the intensity is much lower than that emitted by electrons because the intensity decreases proportionately with the ratio of the squares of the particle masses. Thus the bremsstrahlung produced by protons is about  $(1800)^2$  times less intense and is negligible compared to the other sources of background (Ref 2:9).

Fig. 4 depicts a typical energy spectrum including characteristic x-ray peaks, scatter, and background.

#### Sources of Excitation

Photons, electrons, and protons are the most commonly used sources of fluorescent x-ray production. Photons are emitted by radioactive isotopes or produced in x-ray tubes

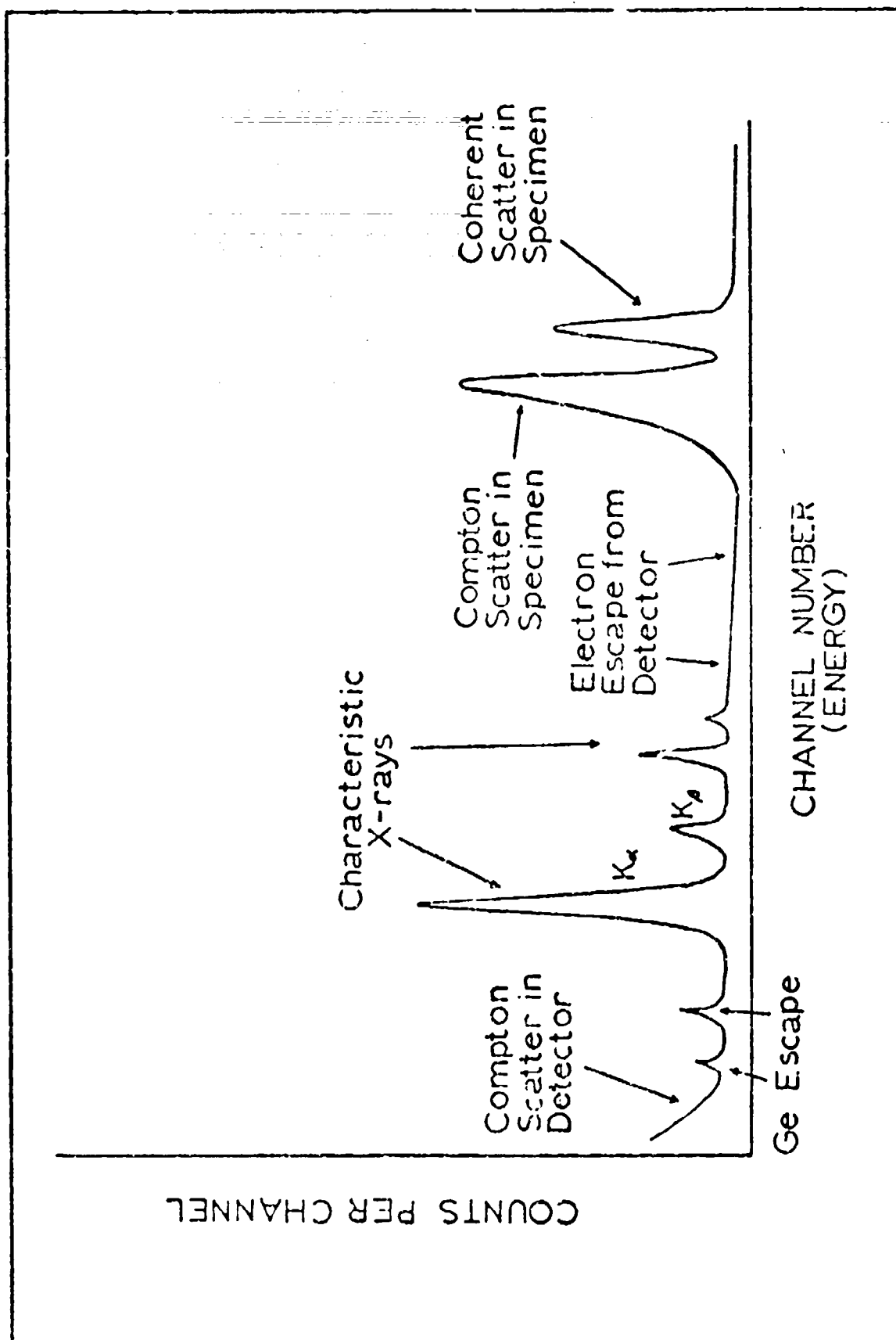


Fig. 4. Typical Energy Spectrum

by bombarding elemental targets with electrons, and electrons and protons can both be used directly to excite characteristic x rays in a specimen. Fig. 5 shows the relative efficiency of these three sources for x-ray production and each source is discussed individually in the following sections.

Radioisotopes. It can be seen in Fig. 5 that in general, photon excitation is the most efficient method of x-ray production. Photon emitting radioactive isotopes are used extensively in energy dispersive spectrometry, but they have some serious disadvantages. Most isotopes emit a variety of different energy photons and particles which result in numerous scatter peaks that can obscure the characteristic spectrum. The major disadvantage of radioisotope use though is their low activity and the long counting times required to collect data. High intensity sources with activities equal to or greater than one curie are available, and would reduce counting times, but they are hazardous to handle and difficult to store when not in use.

Electrons. Electron excitation has become more common with the introduction of electron microprobes, scanning electron microscopes (SEM), and transmission electron microscopes (TEM). Because these instruments use extremely small electron beams to excite a very small volume of the sample, the proportionality between mass concentration and relative x-ray intensity is found to be generally valid and can yield an accuracy of 1% (Ref 1,4). The SEM, for example, produces a beam less than 100 angstroms in diameter, and currents in the  $10^{-12}$  A range (Ref 24,4). The primary disadvantage of

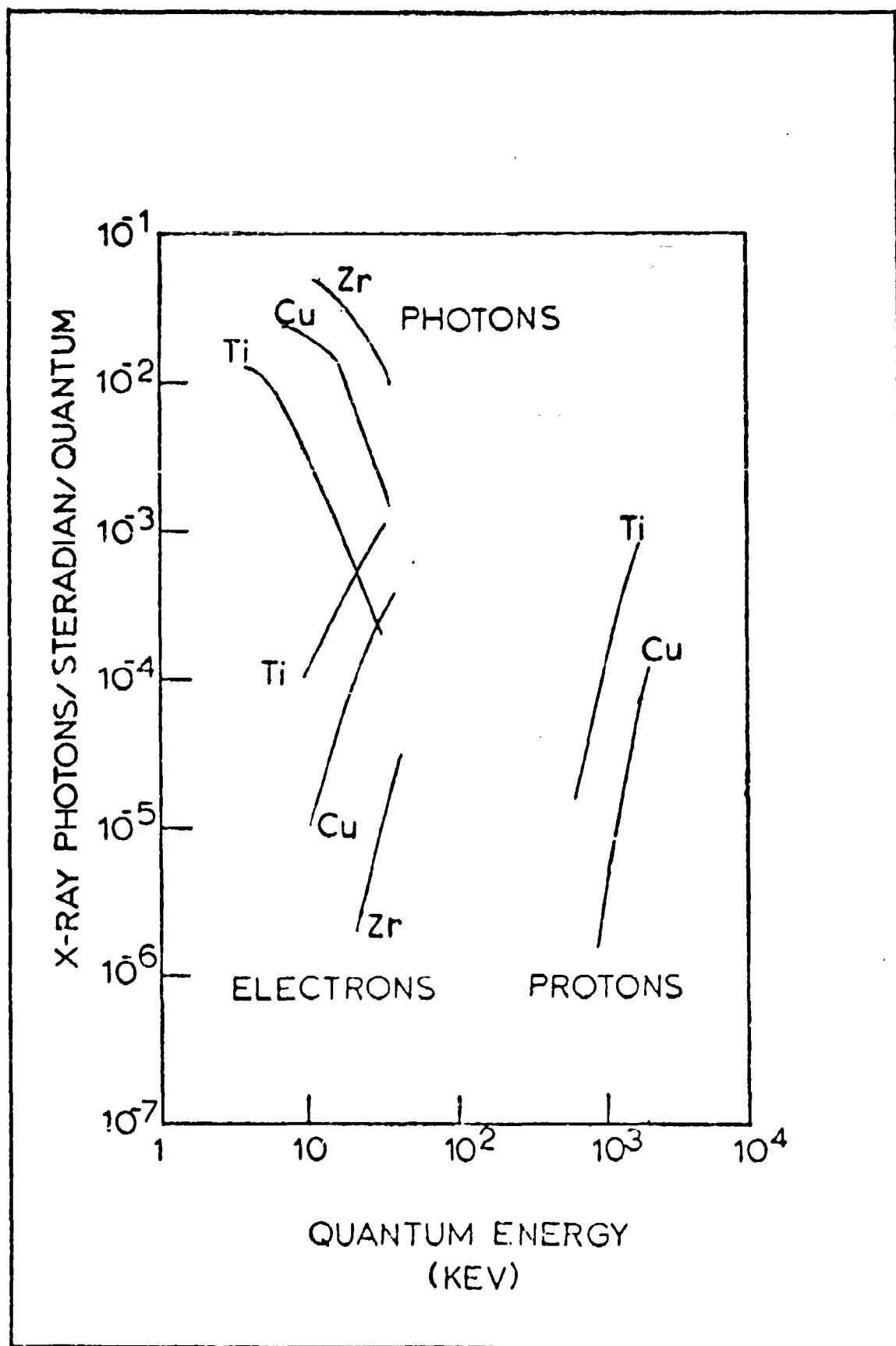


Fig. 5. Total X-ray Yields for Excitation by Electrons, Protons, and Primary X rays (Ref 1:22)

electron excitation is the large amount of bremsstrahlung produced from the deceleration of electrons by inelastic collisions in the sample. Quantitative analysis of low concentrations is difficult without some method of stripping this continuous background.

Protons. Protons show the most promise for use in trace analysis because of the absence of significant bremsstrahlung. Concentrations as low as  $10^{-11}$  g have been reported using 1.5 MeV protons and predictions of detection sensitivity as low as  $10^{-15}$  g have been made (Ref 16:143). Some disadvantages of proton excitation are the expensive equipment required, and the fact, shown in Fig. 5, that production efficiency comparable to electron excitation requires proton energies 100 times higher than the corresponding electron energies.

Fig. 5 can be used to make some other comparisons. The efficiency of photon production by other photons reaches a peak at an energy just above an element's absorption edge and then falls off rapidly as the exciting energy increases. On the other hand, the production efficiency of charged particles is lowest at the absorption edge, and then increases rapidly with increasing particle energy. The crossover observed in the photon and electron curves for titanium gives an indication of when one method is preferred. Electron excitation has been shown to be more sensitive for elements below an atomic number of 30 while photon excitation becomes the more sensitive source above 30 (Ref 28:124).

X-ray Tubes and Electron Guns. X-ray tubes and electron

guns combine some of the advantages of both electron and photon excitation. The photons produced by electron bombardment of target foils can be used to excite specimens with much greater intensity than radioisotopes. The output of an x-ray tube or gun can be controlled by varying the accel rating voltage and electron beam current, and the x rays produced depend on the element used for the anode or target. The spectrum of an unfiltered tube can be almost entirely bremsstrahlung, while transmission-type anodes produce up to eighty-five per cent characteristic radiation. The thickness of transmission targets can be increased to further reduce the transmission of bremsstrahlung, since an element is an efficient filter for its own radiation. But an optimum of three to five half-thicknesses has been reported for transmission anodes, and at thicknesses greater than this too much of the characteristic radiation is attenuated, resulting in greatly reduced intensity (Ref 15,3).

The use of secondary targets which are shielded from the electron beam and are excited by x rays and bremsstrahlung from the primary target is another method for reducing the continuous background. It cannot be eliminated completely because a significant amount of the bremsstrahlung will scatter from the secondary target rather than excite it.

A better method of purifying the source radiation is with the use of balanced filters, sometimes called Ross filter pairs. The procedure is to adjust the thickness of two filters of different elements, so that their transmission of

x rays is nearly equal except for a narrow energy band between their absorption edges. For example, a pair of cobalt and iron filters have a pass band between 7.11 keV and 7.709 keV, which are the absorption edges. This will allow nickel  $K_{\alpha}$  x rays (7.47 keV) to be separated from nickel  $K_{\beta}$  x rays and others close in atomic number to iron and cobalt. The x rays in the pass band are isolated by measuring the radiation from the specimen through first one filter and subtracting from it the radiation from the specimen measured through the second filter. Fig. 6 shows the transmission characteristics of nickel and copper filters. According to J. R. Rhodes (Ref 26;266), to balance the filters at a given energy, their transmission must be equal for that energy so that

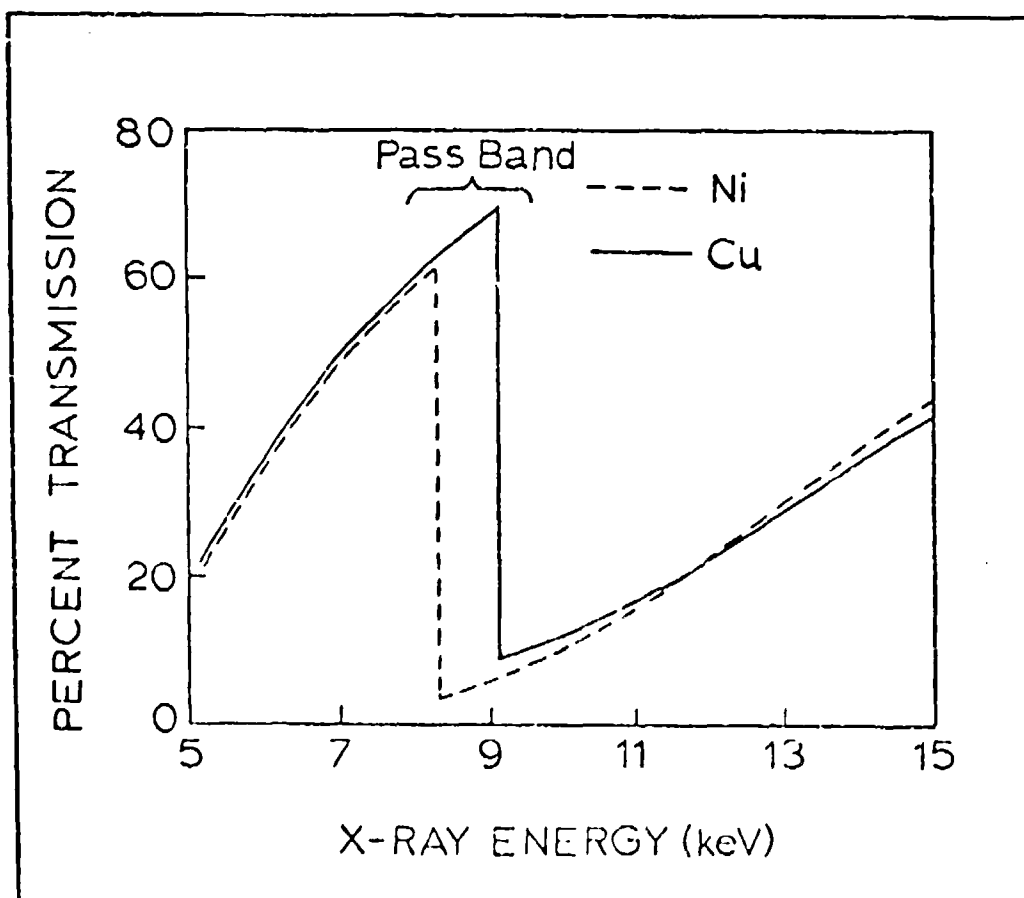


Fig. 6. X-ray Transmission Through Balanced Filters of Copper and Nickel (From Ref 23;266)

$$e^{-(\mu_a M_a)} = e^{-(\mu_b M_b)} \quad (4)$$

or

$$M_a/M_b = \mu_b/\mu_a \quad (5)$$

where  $\mu$  is the mass absorption coefficient and  $m$  is the mass per unit area of elements a and b. The optimum value of  $m$  is given by

$$M_{\text{opt}} = \frac{1.5 \pm 0.5}{(\mu_2 - \mu_1)} \ln \frac{\mu_2}{\mu_1} \quad (6)$$

where  $\mu_1$ , and  $\mu_2$  are the absorption coefficients at the top and bottom of the absorption edge of the element (Ref 26,267).

### Electron Range

When using electrons to excite target foils or excite specimens directly it is desirable to be able to estimate their range or depth of penetration. Electrons do not have definite ranges or straight line paths because of multiple scattering interactions with atoms and orbital electrons, and the straggling caused by large energy losses in collisions with other electrons. The range is defined as the total distance the electron penetrates parallel to its initial direction and is determined empirically (Ref 25,15). The relationship given by Katz and Penfold is

$$R = 412 E^n \text{ (mg/cm}^2\text{)} \quad (7)$$

where  $E$  is the energy of the electron in MeV and  $n$  is given



by

$$n = 1.265 - 0.094 \ln E \quad (8)$$

for values of E between 0.01 MeV and 3 MeV.

### Matrix Effects

The intensities of characteristic x rays emitted from a substance which is a mixture of several elements will not always reflect the concentrations of the elements present. Absorption and enhancement effects occur which modify the relative intensities. When the characteristic x rays of element A have sufficient energy to excite the characteristic x rays of element B, the relative intensity of element B is enhanced while absorption reduces the intensity of element A. If many elements are present in the matrix, these effects can be very complex. Some elements such as copper and nickel do not have characteristic x-ray energies that will excite each other and enhancement and absorption are not observed.

In any quantitative analysis of a substance, matrix effects, if present, must be either eliminated entirely or determined precisely. One method of eliminating matrix effects is to dilute the substance of interest and deposit it as a very thin, uniform film on a thin sample support. With the atoms greatly separated and in a very thin layer, it is assumed that no interaction can occur and a direct linear proportionality between mass per unit area and intensity will exist (Ref 9:1). The intensity is given by Gunn as

$$dI = C \csc \phi_1 I_0 e^{-(\mu_1 \csc \phi_1 + \mu_2 \csc \phi_2) \rho x} dx \quad (9)$$

where

$C$  = constant of proportionality

$I_0$  = intensity of the incident radiation

$\phi_1$  = the angle of the incident beam to the sample surface

$\phi_2$  = the angle of the emergent beam to the sample surface

$\mu_1$  = absorption coefficient of the incident beam

$\mu_2$  = absorption coefficient of the emergent beam

$\rho$  = sample density

$x$  = sample thickness

If the sample is very thin, no absorption will occur, the exponential term is unity and

$$\Delta I = C \csc \phi_1 I_0 \Delta x \quad (10)$$

If the area of the deposit is homogeneous and  $N$  represents the number of atoms of the element in the deposit which fluoresce, then

$$\Delta N \propto \Delta x \quad (11)$$

and

$$\Delta I = C' \csc \phi_1 I_0 \Delta N \quad (12)$$

The proportionality will remain valid as long as absorption in the sample is negligible (Ref 9:2).

This relation is particularly useful in trace analysis where low concentrations are achieved using solutions or diluted specimens deposited in very thin layers. In this case, matrix effects can be ignored.

### III. EQUIPMENT

#### Detector-Analyzer System

The equipment used in this work to detect, display, and store the x-ray spectra is typical of recent energy dispersive systems. A schematic diagram of the system components and their arrangement is shown in Fig. 7. The main components are described in the following sections while a complete list of all the equipment and the optimum control settings can be found in Appendix A.

Detector. The detector used in this experiment was a General Electric Series 411 High Purity Germanium Spectrometer mounted horizontally in a cryostat. The germanium has a  $30 \text{ mm}^2$  active area and a 4 mm sensitive depth. Because of the exceptionally high purity ( $5 \times 10^{10}$  atoms/cm<sup>3</sup>), lithium-drifting is not required and temperature cycling will not damage the detector. However, the detector is maintained at liquid nitrogen temperatures to reduce noise in the field-effect transistor (FET) and improve resolution. An attached ion pump maintains the detector vacuum at  $10^{-5}$  Torr or less. The detector preamp features the advanced low noise, pulsed optical feedback system.

The detection process begins as x rays enter the sensitive area of the germanium through a half-mil beryllium window. Each 2.98 eV of energy deposited produces an ion pair. This charge is collected by an applied negative bias of 660 volts, and is proportional to the energy of the absorbed

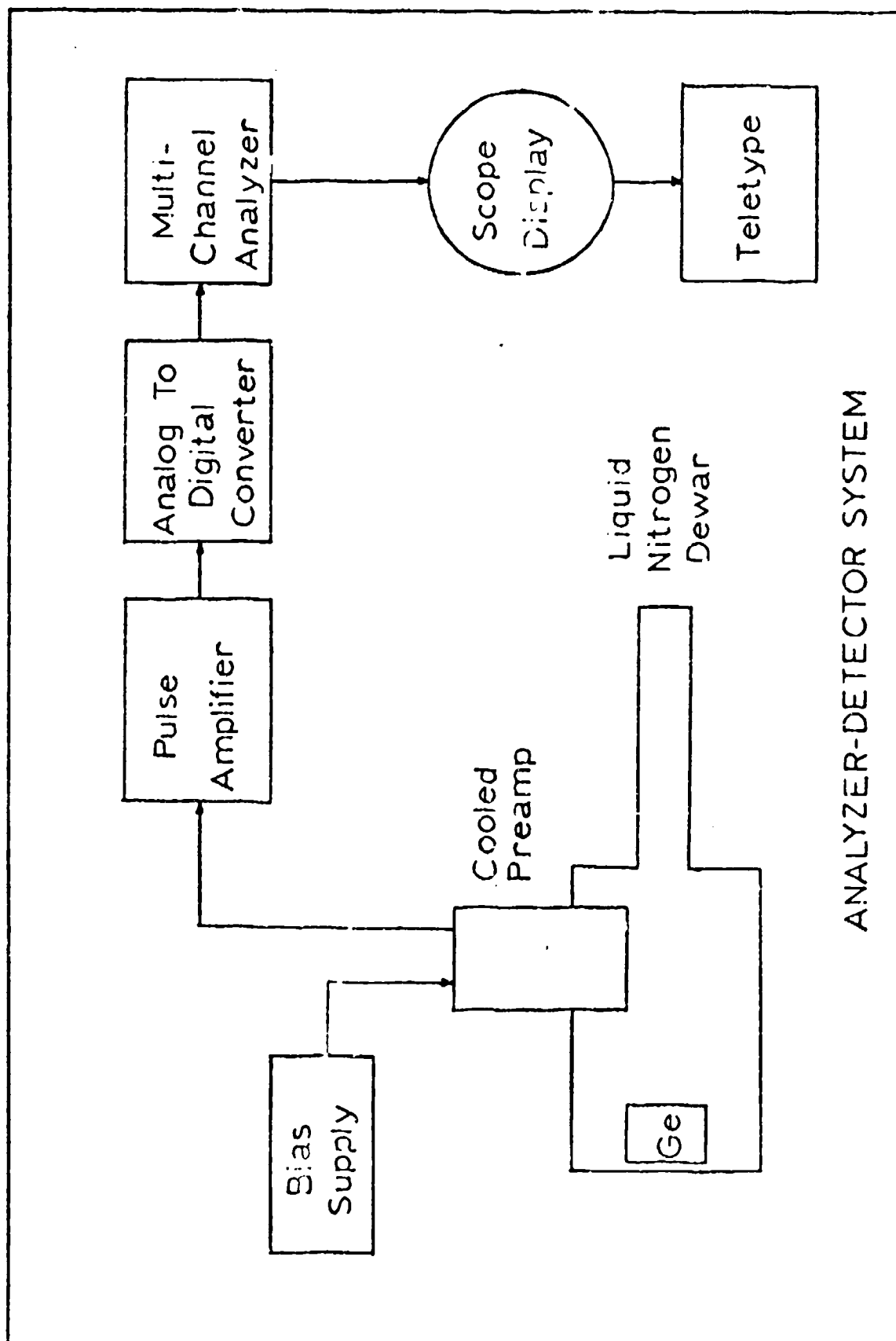


Fig. 7. Detector-Analyzer System

x ray. The charge is amplified by the FET preamp whose output is a series of steps, each proportional to an x-ray energy. The baseline voltage of the preamp is reset after each series of events by the optical feedback system. The preamp signal is then amplified again, filtered, and shaped into pulses proportional in height to the energies deposited. These pulses are then examined by the multichannel analyzer and stored in memory addresses corresponding to the measured energies.

The resolution of the detector determines its ability to separate elements close in atomic number. The standard measure of resolution is the full width at half-maximum (FWHM) and minimizing its value is a primary concern in detector design. A FWHM of 200 eV was obtained with this detector measured for the 6.4 keV x ray of iron.

Multichannel Analyzer. The multichannel analyzer was a Nuclear Data Series 2200 modular system with an integrated tape transport for storage and retrieval of spectral data. The spectrum was displayed on a Hewlett-Packard oscilloscope and printed output obtained from a teletype. The system memory provides selection of 512, 1024, 2048, or 4096 channels.

#### Scattering Chamber

A commercially available Ortec Model 3703, 17-in. diameter scattering chamber was used for the experiments. The chamber is forged, annealed aluminum one-inch thick with entry and exit ports plus two accessory ports in the sides.

It is mounted on a welded steel stand equipped with leveling screws on each of the three legs. A collimating tube for the entry port, a Faraday cup, and a spun-aluminum dome cover were also provided by the manufacturer. The bottom of the chamber has two more accessory ports, electrical feed-throughs, and a vacuum bleed valve.

The chamber is equipped with a unique positioning mechanism which includes two slotted, rotating arms and a rotating center sample holder. Each rotating element is independently controlled by a worm drive operated externally with a crank-type handle. The handle gives  $3^\circ$  of rotation per turn and a vernier scale allows positioning accurate to  $0.1^\circ$ .

The chamber is evacuated through an accessory port on the bottom by an oil-diffusion pump with a liquid nitrogen vapor trap. Using the factory cover, a vacuum of  $10^{-7}$  Torr was possible, but with the clear plexiglass cover used during the experiments, the minimum vacuum achieved was only  $10^{-6}$  Torr. The plexiglass apparently outgasses and the substitution of a glass cover would undoubtedly improve the vacuum.

The blank on one of the side accessory ports was removed and replaced by an aluminum collar with a  $3/8$ -in. diameter, one-mil beryllium window. The collar allows the detector window to be aligned with the chamber window so that x rays from the chamber can enter the detector. The collimating tube was removed from the entry port and an electron gun was attached to the chamber. The chamber and associated components are shown in Fig. 8.

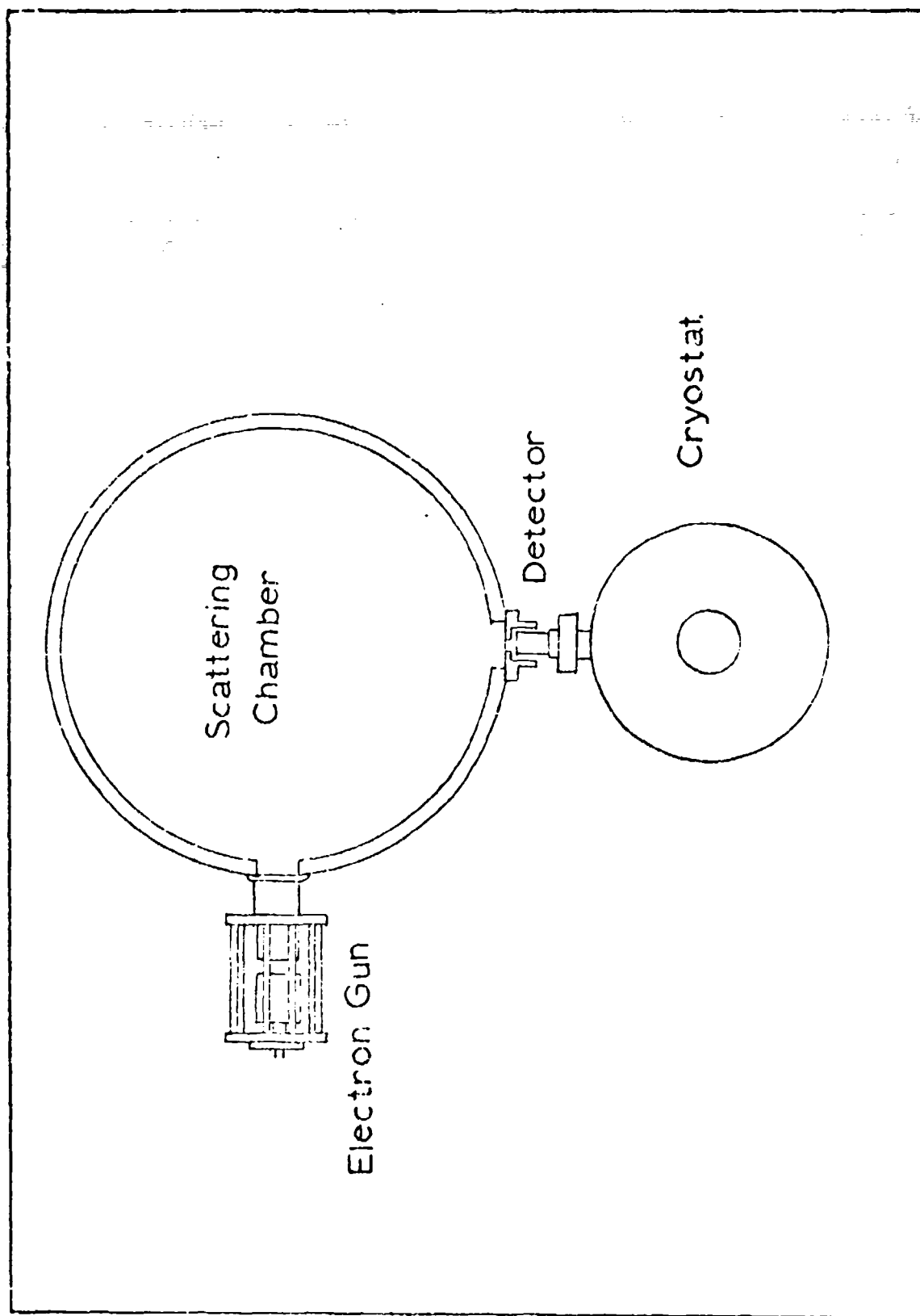


Fig. 8. Arrangement of Scattering Chamber, Detector, and Electron Gun



... electron gun is based on a design originally proposed by K. Steigerwald called a focusing cathode. The specific gun used in this experiment was designed by Dr. R. L. Hengehold of the Air Force Institute of Technology using data on system parameters reported by F. W. Braucks (Ref 4:212).

This gun is very versatile and could have several applications in addition to the energy dispersive x-ray spectrometry investigated in this experiment. It has several advantages over conventional electron guns and x-ray tubes. The gun does not have to be kept evacuated when it is not operating, and therefore does not have to be isolated from the scattering chamber when the chamber is opened to change samples or targets. Any element that can be obtained as a foil can be used as a target allowing selective x-ray excitation of specimens. It can also be used without targets for direct electron excitation. Most electron guns must be kept continuously evacuated to prevent oxidation damage to their components, while x-ray tubes are permanently sealed and cannot be modified. The cost of the Steigerwald gun is much less than the cost of maintaining a variety of x-ray tubes with different anodes. In addition, the source of electrons in this gun is a 0.005-in. thoriated tungsten filament which is easily replaced.

An important feature of the gun is the focusing capability. By adjusting the vertical position of the filament

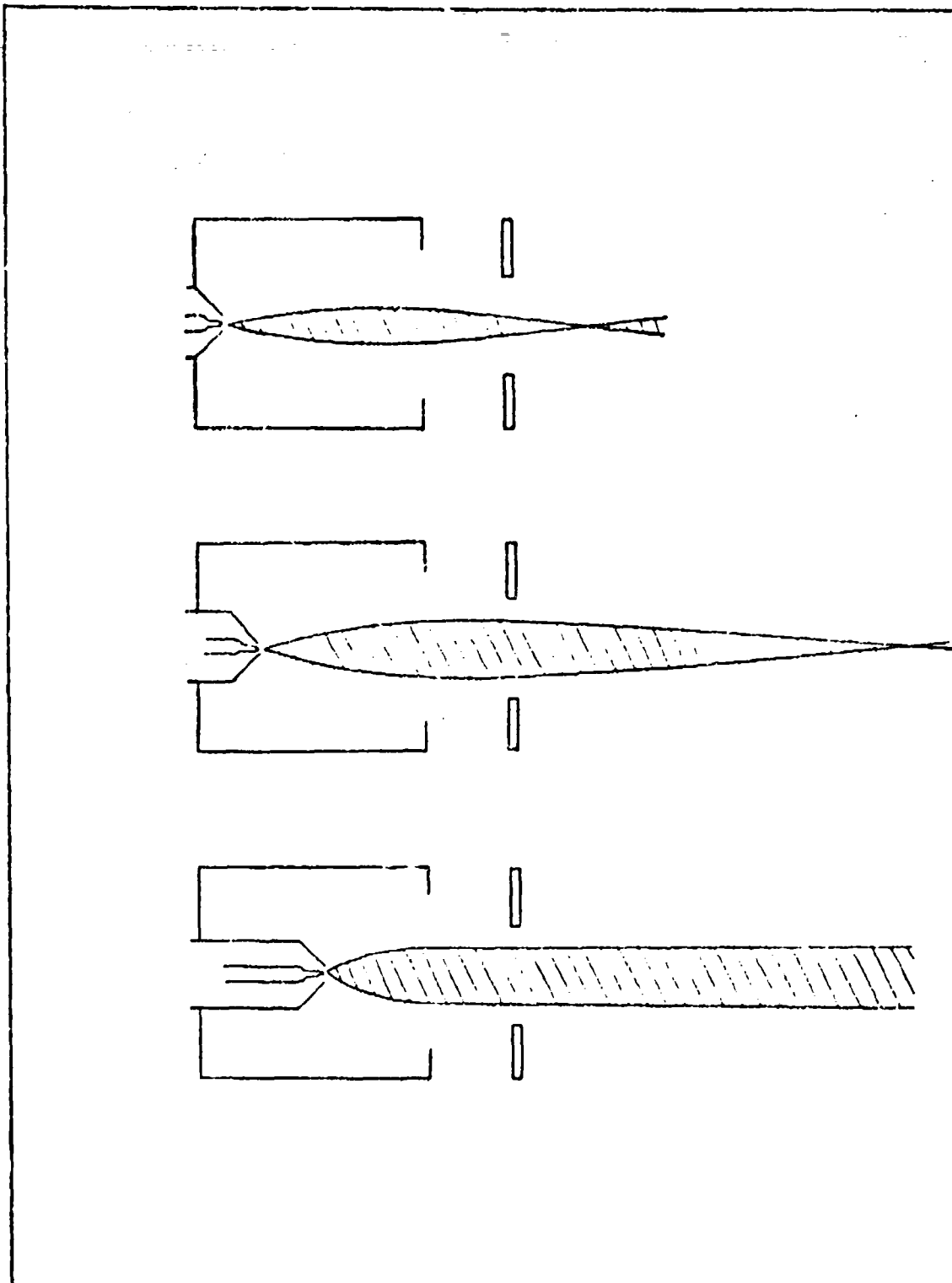


Fig. 9. Effect of Filament Position on Electron Beam Characteristics (From Ref 2,248)

in the focusing cathode, the position of the focal point or point of minimum beam diameter can be selected. Beam diameters as small as 0.02 mm are possible at the focal point. A divergent or unfocused beam may also be selected and in practice the electron beam diameter can be varied from several millimeters up to an inch by adjusting the focusing voltage regardless of the geometrical parameters. However, the minimum beam diameter will be obtained only at the distance and system parameters predetermined by the filament position. The effect of filament position on beam characteristics is shown in Fig. 9.

Construction of the gun was accomplished in the school machine shop from materials which included aluminum stock for the majority of the components, stainless steel for the filament holder, a glass tube to separate the high voltage sections, and plexiglass rods to join the entire assembly. Fig. 10 is a detailed cutaway diagram of the gun assembly.

The gun is operated by first heating the filament which emits electrons that are then accelerated through a potential difference. The beam is then focused by negatively biasing the focusing cathode with respect to the filament. The larger the negative bias, the greater is the pinching or focusing effect on the electron beam. In this experiment it was desirable to maintain the scattering chamber at ground potential, so the high voltage required to accelerate the electrons was applied to the filament and focusing cathode assembly. This arrangement made it necessary to float the filament current supply and focusing voltage supply.

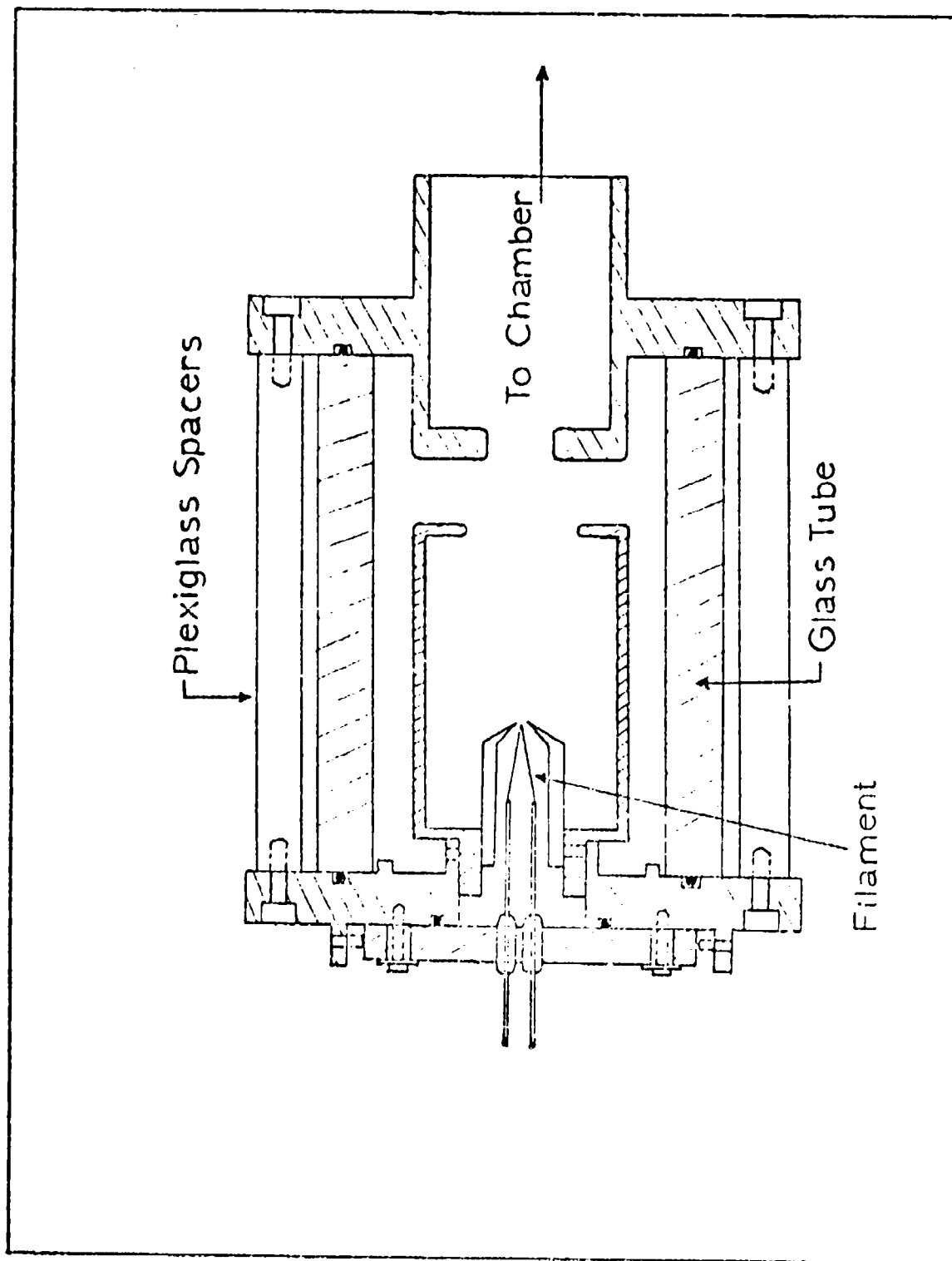


Fig. 10. Electron Gun

Batteries were selected as the simplest solution to these power requirements and no difficulties were encountered during their use. A six-volt rechargeable automobile battery was used to supply the filament current and was adjusted using a 3.1 ohm slide wire resistor connected as a rheostat. The output was very stable and recharging when necessary could be accomplished overnight. A 300-volt dry cell battery was used to supply the focusing voltage. The output was selected by a one megaohm potentiometer that kept the current output low and increased the battery life. The batteries and electrical wiring were housed in an insulated container equipped with non-conducting control rods for adjustment of filament current and focusing voltage.

The high voltage was supplied by a Spellman 60 kV regulated power supply. Fig. 11 is a schematic diagram of the electrical circuits for the gun, high voltage supply, filament supply, and focusing voltage supply.

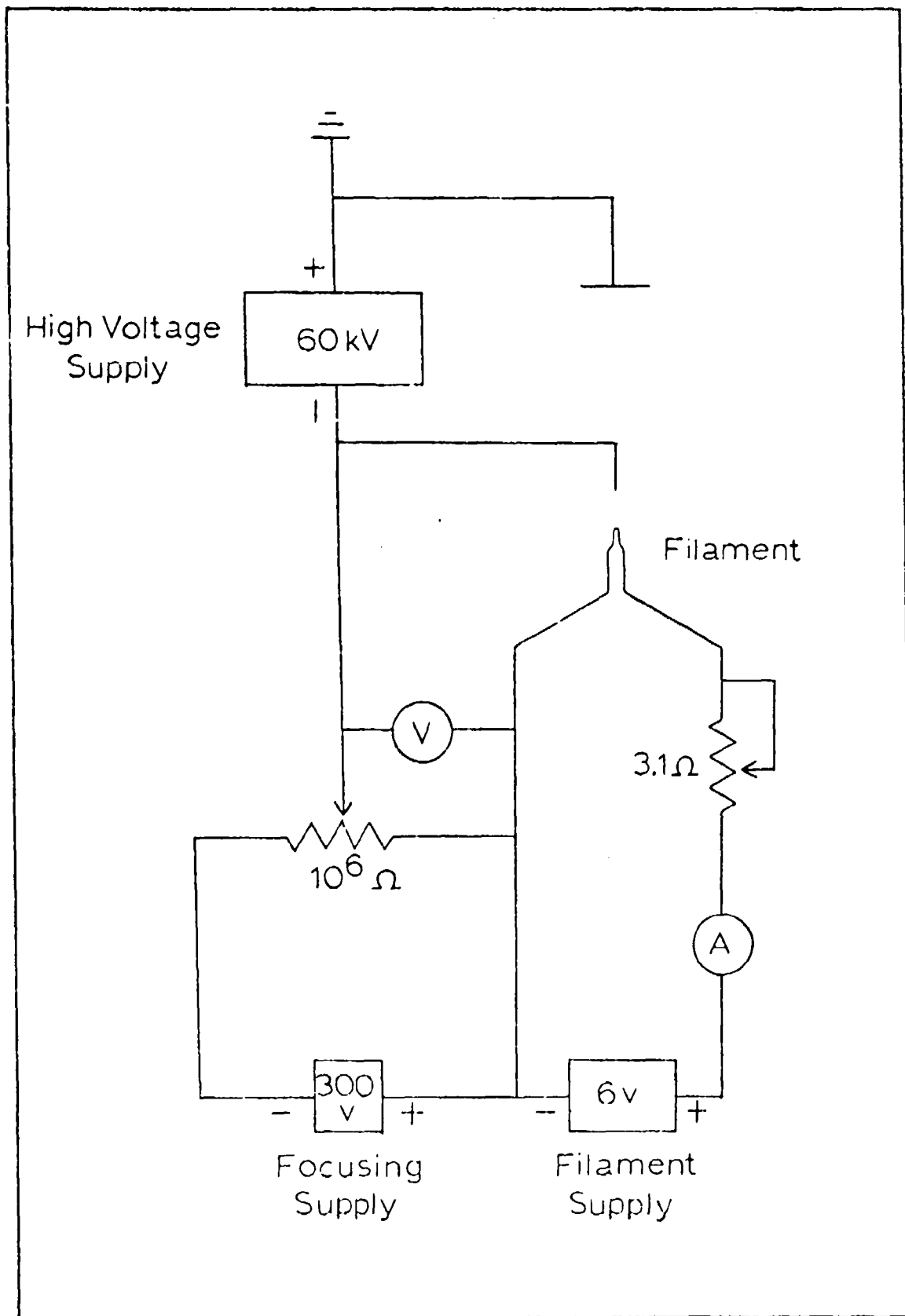


Fig. 11. Circuit Diagram for the Electron Gun

#### IV. EXPERIMENTAL PROCEDURE

The experimental procedure is described in this section in three parts. Part one deals with the initial set-up and equipment calibration plus the determination of the operating characteristics of the system. The second and third parts describe the experiments performed using both transmission x-ray excitation and direct electron excitation. Target foil selection and sample preparation are discussed as they apply to each experiment.

##### Equipment Calibration and Operation

The energy calibration of the detector and analyzer was accomplished by exciting a wide range of pure elements and recording the channel location of the peaks. A computer program was used to fit the data to a polynomial equation and provide a printout listing each channel and its energy. The equipment drifted only slightly during the experiments and just one calibration was necessary.

The high voltage power supply was rated at 60 kV, but because of the large load created by the electron gun and associated components, only 40 kV were available at maximum output. The full 40 kV was used without experiencing electrical breakdown or arcing in the electron gun. The electron gun emitted beam currents from 1  $\mu$ A to 300  $\mu$ A using less than 2A of the total 2.8A available from the 6v battery. The beam could be focused or pinched off completely throughout these current and voltage ranges using less than half of the 300v

capacity of the focusing supply.

The high voltage connection between the power supply and the electron gun was made using well-insulated RG-8/U cable which constituted no hazard even at high voltages. However some of the other wires, particularly the longer lengths, were attracted to each other or grounded components as the voltage was increased, and constituted a possible hazard. These problems were eliminated by shortening the wires as much as possible and separating them with wooden spacers. The electron gun was shielded from accidental contact by a plexiglass enclosure, as were all uninsulated connections, to prevent personnel injury.

The correlation between x-ray production and electron gun output was determined by measuring the change in x-ray intensity as beam current was varied while holding the accelerating voltage constant. The same measurement was then made by varying the voltage and holding the current constant. The observed behavior was compared to predicted values and the results are discussed in Section V.

Before performing specific experiments with x-ray or electron excitation, the geometrical arrangement which provided the optimum characteristic intensities and minimum background was sought. The electron source and detector were maintained  $90^\circ$  apart throughout the study. The variables investigated included the source-sample arrangement, shielding of the sample-detector path, and shielding of the target to reduce bremsstrahlung and scattered radiation. The effect



of target thickness on the transmitted spectrum used to excite the specimens also was examined.

Various collimating and shielding arrangements were tried while exciting characteristic x rays in large specimens. It was noted that despite a good peak to background ratio and low observed level of bremsstrahlung in the spectrum, the peak resolution was very poor. It was suspected that this was caused by low energy bremsstrahlung that was overloading the amplifier, but was not reflected in the live time. This had arisen in previous work (Ref 12:25), and the use of Scotch tape as a low Z absorber had eliminated the problem. This solution was tried, and by placing five layers of ordinary Scotch tape over the detector window, the resolution was restored.

The apparently good background reduction achieved when exciting the thick specimens was inadequate when analyzing concentrations in the microgram range. The shielding arrangement had to be revised to permit detection of  $0.1 \mu\text{g}$  concentrations above the background. There were two critical areas for background reduction. The first was at the detector window. The path from the sample to the detector had to be shielded from scattered radiation while admitting characteristic sample x rays transmitted through a small solid angle. Of the two arrangements tried, the long, graded collimator was the least successful apparently because of scatter from the inside of the tube. The better arrangement is shown in Fig. 12 and proved to be satisfactory for all the experimental

work.

The most critical area was the target foil. Because of the size and shape of the scattering chamber, large amounts of bremsstrahlung were scattered from the sides and back of the target foils and entered the detector. Backscattered electrons probably also contributed to the general level of background radiation by interacting with the chamber. This continuous background was reduced at least tenfold by enclosing the target and electron beam in a graded tube. The specimen was excited through a half-inch opening in the end of the tube, and for optimum reduction in background, the tube had to be extended all the way to the entry port. A slot was cut in the top of the tube to insert targets and even this had to be kept covered because of the large amount of radiation scattered from the target at  $90^\circ$  to the electron beam. The complete arrangement of the chamber for transmission x-ray excitation is shown in Fig. 12.

Measurements of radiation dose were taken around the chamber and levels as high as 200 mr per hour were observed at high potentials with the target unshielded. These levels were reduced to practically zero with the target in the shielding tube.

#### Transmission X-Ray Excitation

Target Selection. The ability to change targets and selectively excite different ranges in the energy spectrum is one of the advantages of the electron gun. The range of excitation energies available is limited by several factors.

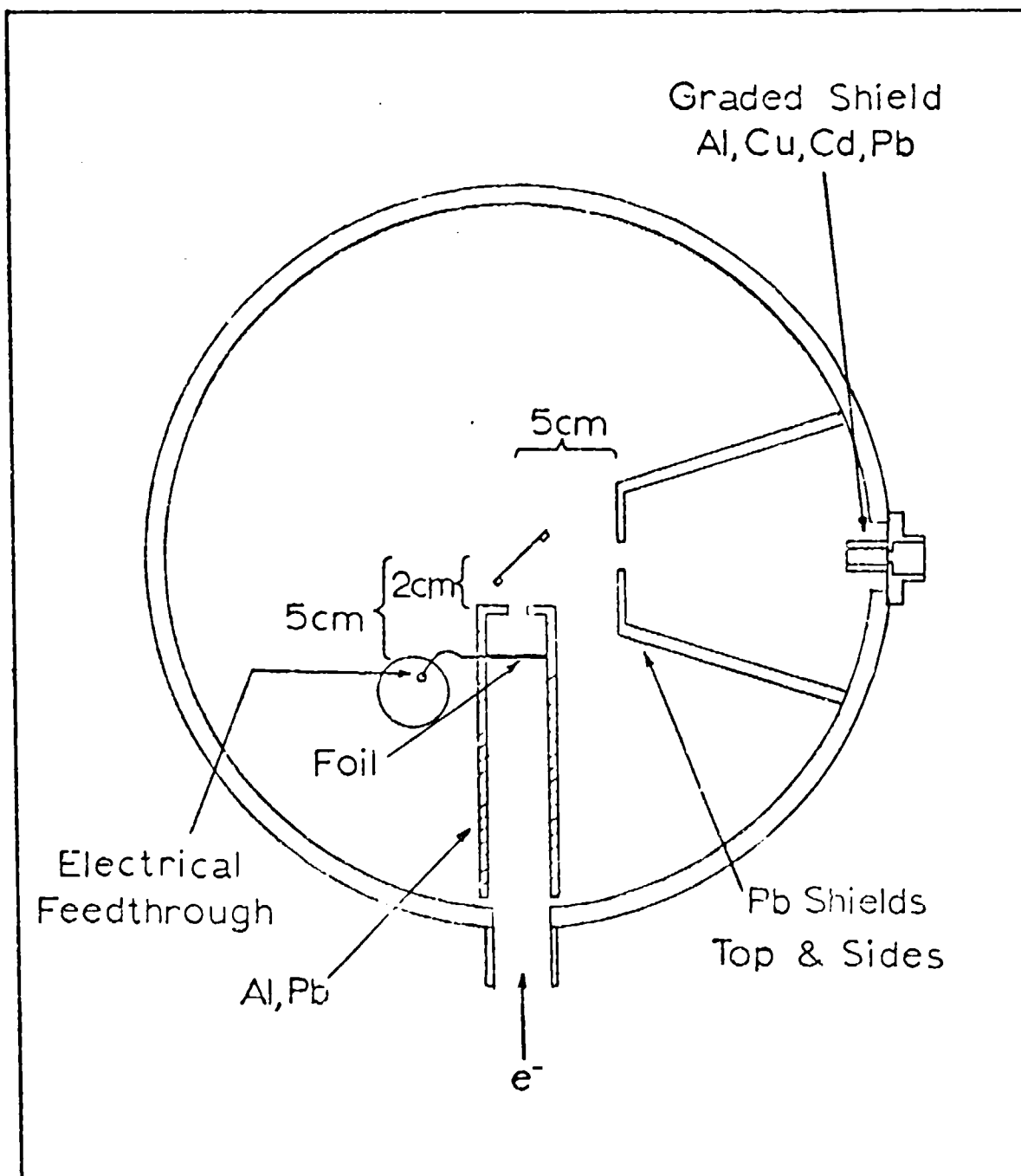


Fig. 12. Optimum Geometry for Transmission Foil Excitation

First the desired element must be available as a thin foil. Secondly, the melting point and thermal conductivity must be high to withstand the heat energy created by the electron beam. Elements such as lead, tin, or cadmium, are not suitable usually because of their low melting points.

In this work it was essential to the accuracy of the results to be able to monitor the electron beam current and keep it constant during the experimental runs. This was done by measuring the current directly from the target foil with a microammeter, utilizing the electrical feedthrough in the bottom of the chamber. To do this, the target and shielding assembly had to be insulated from the chamber which was at ground. With the chamber evacuated, the only heat loss would be through radiative transfer and the rest would have to be absorbed by the target assembly. Some simple calculations illustrate the problem. At 35 kV and 200  $\mu$ A, the beam will deposit 7 J/sec in a molybdenum target. If the radiative loss is given by

$$Q_{\text{RAD}} = \sigma \epsilon T^4 \quad (13)$$

where

$\sigma$  = Stefan-Boltzman constant

$\epsilon$  = emissivity of molybdenum

T = temperature in degrees centigrade

The temperature at which energy input and radiative loss are equal is 8000° C, well above the melting point of molybdenum.

However, a molybdenum foil placed in a lead-covered aluminum tube was excited by a 35 kV, 200  $\mu$ A electron beam for up to 4000 sec during this study with no adverse effects. This is explained by the large mass of the whole assembly and high conductivity of the foil. The heat is conducted efficiently to the lead and aluminum which absorb it. The temperature increase can be computed from

$$U = MC_v T \quad (14)$$

where

$U$  = heat input in calories

$M$  = mass

$C_v$  = specific heat

$T$  = temperature increase in degrees centigrade

With a heat input of 7 J/sec, 6692 calories will be deposited in 4000 seconds. With a mass of 500 g and specific heat of 0.08 cal/g- $^{\circ}$ C, an increase in temperature of only 167 $^{\circ}$ C will result. This estimate is slightly high because the specific heat of aluminum is greater than that used in the computation. Continuous runs were limited to approximately 4000 seconds to prevent excessive heat build-up. It is obvious that an insulated target foil weighing several grams by itself would not withstand large power inputs.

Transmission target foils were sought with a wide range of K x-ray energies and thicknesses. The optimum thickness was found to be three half-thicknesses based on the experimental geometry and length of the path between the sample and

detector. Thicker foils produced too low a count rate when exciting samples of low concentration. Time did not permit ordering foils from a commercial supplier and it was difficult to obtain the desired foils in the exact thicknesses required. With some elements it was possible to reduce thick foils by etching or rolling.

Sample Preparation. The emphasis in the transmission x-ray excitation was on the quantitative determination of low elemental concentrations. Previous studies have been made using liquid solutions deposited on mylar film and evaporated (Ref 8:921). Standard 1000 ppm solutions containing dissolved metal salts were obtained. These could be further diluted to provide any concentration below  $10^{-4}$ g. To deposit larger concentrations, a time consuming process of successive deposits and evaporations was required, and instead, undissolved chemical salts were obtained and additional standard solutions of  $10^4$  ppm and  $10^5$  ppm were made. The same chemical compound was used in all standard solutions of the same element so as not to introduce additional uncertainties in the data.

Mylar makes an excellent sample support because of its durability and the low amount of background it contributes to the spectrum. The solutions were deposited on 0.25-mil mylar sheets with micropipets and allowed to evaporate under a heat lamp. However, the solutions deposited directly on the mylar were not uniform. The low concentrations had a tendency to shrink into very small areas as they dried while the high

concentrations were spread out much more. Better results were obtained by evaporating a small amount of a wetting agent on the mylar before depositing the sample solutions. The solutions then dried more uniformly and were confined to fairly constant areas. The best procedure used was to deposit 100  $\lambda$  (0.1cc) of the wetting agent on the mylar and let it dry. Then 100  $\lambda$  of the sample solution was deposited over the wetting agent producing a sample area about one centimeter in diameter when it evaporated.

The weights were calculated by assuming the densities of the solutions to be the same as water (1.0 g/cc). A 100  $\lambda$  drop then weighs 0.1 g and if the concentration is 1000 ppm, the drop contains  $10^{-4}$  g of the sample element.

Samples were made using this procedure with concentrations from  $10^{-8}$  g up to  $10^{-2}$  g. The samples had to be carefully handled, particularly the higher concentrations, to prevent the deposits from flaking and falling off the mylar. Samples such as atmospheric dust, blood, and powdered concrete were examined and presented even more of a problem in preparation. Some, such as atmospheric dust, were deposited on the mylar in a slurry of de-ionized water and adhered well when dry. The powdered concrete was fixed to the sample support with a very light coating of vacuum grease which did not contaminate the spectrum. Blood and some other substances which had a tendency to flake when dry could be sprayed with a thin coating of plastic lacquer without affecting the observed intensities.

National Bureau of Standards steels were obtained for use in analysis of solids. These came in rods a half-inch in diameter. Samples were prepared by cutting disks 3/8-in. thick from the rods and turning the faces on a lathe so that all the samples were uniform. Samples of pure elements to be used in the same experiments were machined from solid stock in the same size and shape as the steel disk. Before use in the vacuum chamber they were all cleaned thoroughly with acetone.

Trace Element Analysis. Experimental runs were made to measure characteristic x-ray intensities emitted from samples excited by x rays from transmission foils bombarded by electrons. Samples of each pure element of interest were made from standard solutions in weights from 0.01  $\mu$ g to 0.01 g. The samples were then excited and the intensities recorded. Excitation energies close to the absorption edges of the sample elements were used whenever possible. For example, 2-mil copper foils were used to excite chromium and iron while 5-mil molybdenum was used to excite rubidium and strontium.

Aluminum was tried first as a sample holder. The mylar sample support was held on a thin aluminum frame by applying a small amount of silicon vacuum grease to the edges. The aluminum was not satisfactory, however, because it contained contaminants such as iron and chromium which produced peaks in the spectrum. A frame made from 1/8-in. plexiglass gave better results and no contaminants or increase in scatter were observed. The holder was attached to the center column



of the chamber and could be rotated. The optimum position of the sample was found to be at a  $45^\circ$  angle to both the detector and the excitation source.

Initially, each sample was introduced individually into the chamber. This procedure was time consuming because it took approximately thirty minutes to change samples and re-evacuate the chamber after each run. To save time, a revolving sample holder or carousel was designed which held up to six samples. The carousel was made from aluminum and a small increase in background from contaminants and scatter was observed when it was used. The carousel and its position in the chamber are shown in Fig. 13. The mylar sample support is mounted on a plexiglass holder and suspended from one of the arms on the carousel. When the center column of the chamber and the attached spool are turned, an O-ring stretched between that spool and a similar spool on the carousel turns the carousel and rotates the samples into position.

Most experimental runs were 1000 seconds long using an electron beam current of 200  $\mu$ A and a beam potential of 35 kV. For each weight, three samples of the same element were excited and at least two runs were taken with each sample. The data obtained from exciting the pure samples was used to compile standards relating observed x-ray intensity to weight concentration. Other more complex substances were excited under the same experimental conditions, and analyzed quantitatively by reference to the standards.

Several variables had to be monitored to reproduce the

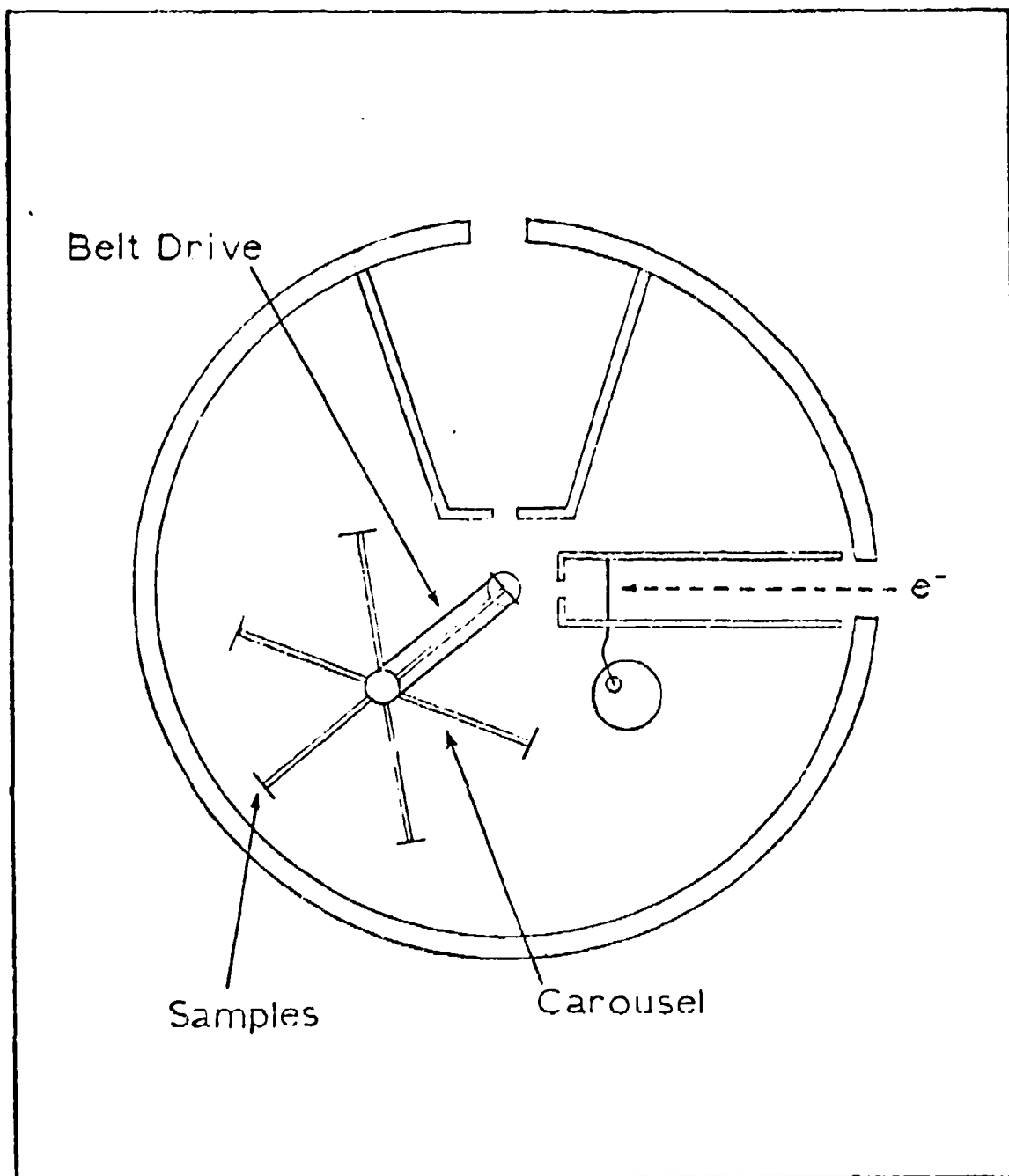


Fig. 13. Carousel Sample Holder

same set of conditions for each run. The electron beam was affected by the earth's magnetic field and its position varied with electron energy. The beam could be observed by dusting the target with a fluorescing powder such as cadmium sulfide, and its position controlled using an ordinary bar magnet. Before a series of runs was made, the beam had to be centered on the target and the position of the magnet noted. The beam diameter was dependent on accelerating potential, focusing voltage, and filament current and all three had to be duplicated for each run in a series. If beam potential and current are held constant as filament current is increased, the beam diameter will decrease. This occurs because the focusing voltage must be increased to keep the beam current constant as more electrons are emitted from the filament. During the experimental runs there was very little variation in the excitation parameters. The high voltage supply was regulated and varied less than one per cent. Once the system had stabilized after a few minutes of operation, the variation in the beam current was less than 5% and it could be monitored and adjusted when necessary during the runs. Small changes in the filament current occurred during the first few minutes of operation as the filament heated up and the resistance changed. The ammeter used to monitor filament current did not have a very sensitive scale and these changes were not always detectable except by the variations they produced in the beam current. This was not critical and could be compensated for by adjusting the focusing voltage to

keep the beam current constant.

Analysis of Solids. An attempt was made to analyze elemental concentrations in steel standards by selectively exciting the elements in the samples to determine matrix correction factors. The assumption was that radiation from an iron target foil would excite only chromium in a matrix containing chromium, iron, and nickel, and that a nickel foil would excite only chromium and iron. By comparing the intensities emitted from the steel samples and intensities emitted from pure elements, empirical correction factors would be computed. Unknowns with the same three element matrix could then be analyzed using these correction factors and their elemental weight fractions determined.

The first technique tried was to excite the samples with radiation transmitted through a 7-mil iron foil to obtain the un-enhanced chromium intensity. This was not successful because a large amount of bremsstrahlung was also transmitted and excited the iron and nickel in the samples which enhanced the chromium intensity. The presence of enhancement was determined by comparing the chromium intensity from the steel to that emitted by a pure sample excited under the same conditions. If matrix effects are not present then the relationship is given by

$$I_{Cr}^m = I_{Cr}^p W_{Cr}^m \quad (16)$$

where  $I_{Cr}^m$  = x-ray intensity emitted by chromium in matrix m

$I_{Cr}^p$  = x-ray intensity emitted by pure chromium

$w_{Cr}^m$  = weight fraction of chromium in matrix m

If the weight concentration computed from the observed intensities is greater than the actual chromium concentration in the sample then enhancement has occurred.

A second technique was used in an attempt to eliminate the transmitted bremsstrahlung. The experimental arrangement is illustrated in Fig. 14. A molybdenum target foil was placed at a  $45^\circ$  angle in a lead-covered aluminum tube with an opening in the side. The radiation produced by electron excitation of the molybdenum is transmitted through the foil and leaves the tube at a  $90^\circ$  angle to the direction of the electron beam. This radiation then excites characteristic x rays in a secondary iron target which, in turn, excites the steel samples. This geometry did reduce the amount of bremsstrahlung but not enough to eliminate excitation of iron and nickel by radiation scattered from the iron secondary target. The proposed experiment was not completed because of the failure to selectively excite the chromium in the steel samples. The enhancement observed in each case is discussed in Section V and compared to results using direct electron excitation.

#### Direct Electron Excitation

Two experiments were attempted in an effort to analyze elemental concentrations in steel standards by direct electron excitation.

Selective excitation of the elements in the sample by varying the electron beam energy was tried first. By

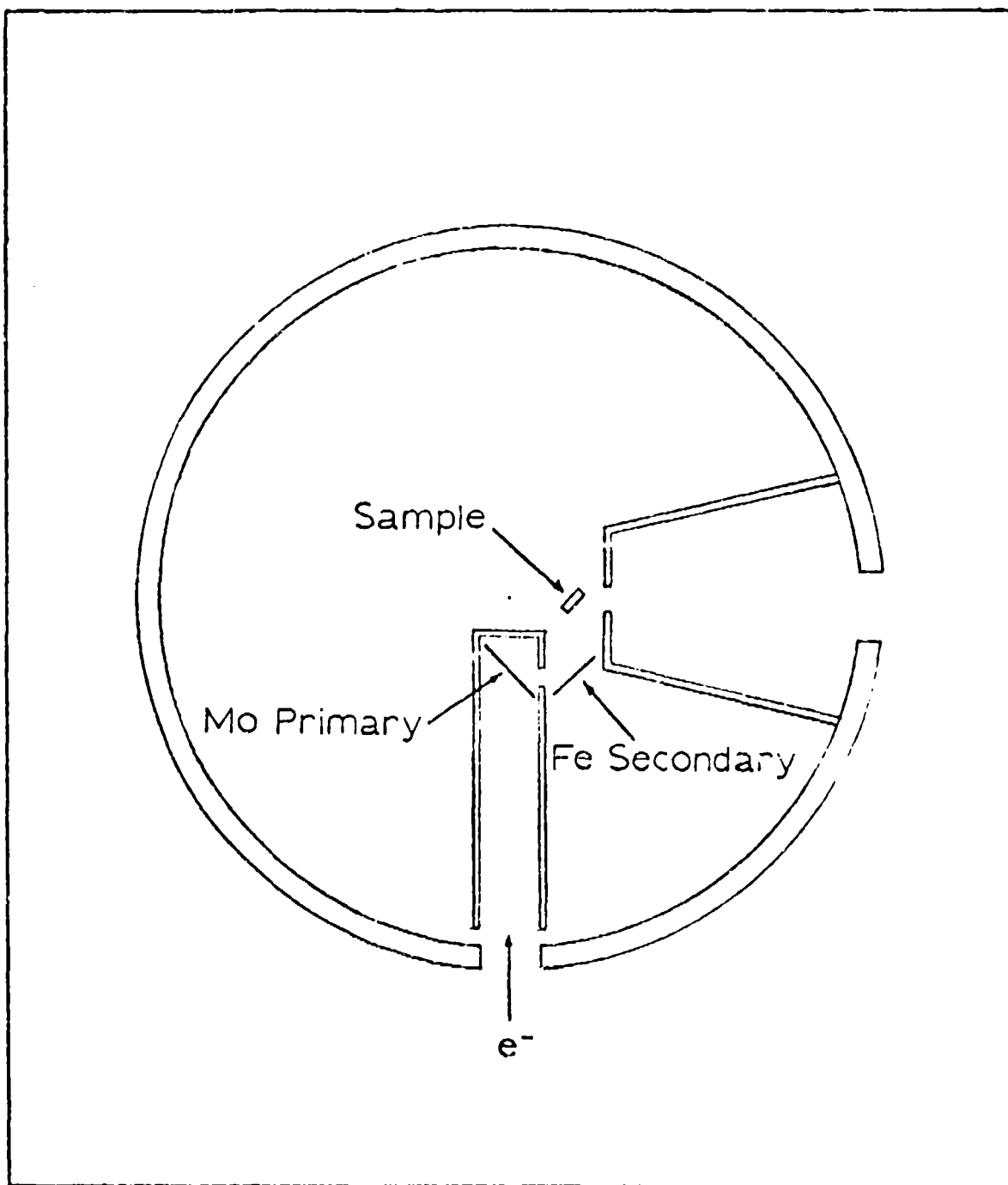


Fig. 14. Chamber Set-up for Excitation of Steel  
Using Iron Secondary Target

adjusting the beam energy so that it was just above the K absorption edge of chromium but below the K absorption edge of iron it was hoped that only chromium would be excited. The chromium was selectively excited but the efficiency of production of x rays by electrons was so low at that energy ( $\sim 6.0$  keV) that the peak was barely detectable above the continuous background and this experiment was discontinued.

The efficiency of production was much better at beam potentials above 15 kV, and the continuous background could be reduced considerably by using a finely focused beam with a very small diameter. The second experiment was to use the focused beam to excite the steel samples and correlate the observed intensities and concentrations by determining the amount of enhancement and absorption present. Since electrons have short ranges it was expected that only the surfaces of the samples would be excited and thus matrix effects would be minimal. The electron range in iron, for example, is only 1.15 microns at 20 kV.

The samples were mounted on the carousel at a  $45^\circ$  angle to the electron beam, and were lightly dusted with CdS so that the beam could be positioned accurately. The sulfur and cadmium were also excited but their peaks did not interfere with the characteristic peaks of the elements in the steel. The experimental runs were all 100 seconds long and the K x-ray intensities of the three elements in the samples were recorded after each run. The beam diameter could be monitored visually and kept constant by adjusting the beam

current which was measured directly from the carousel by insulating it from the chamber with teflon spacers.



V. DATA ANALYSIS AND RESULTSSystem Operation

Since a wide range of electron energies and beam currents were available, their effect on the production of characteristic x rays was investigated to determine the optimum combination for each experiment. The x-ray intensities were measured from pure samples while varying the beam current and holding the accelerating potential constant. Both solids and evaporated solutions were used as samples. Fig. 15 shows the results obtained from a  $10^{-3}$  g chromium deposit excited by copper x rays, and from a large sample of pure copper excited by rhodium. The relationship between current and intensity is linear, but the rate of increase in intensity becomes larger as the concentration of the sample element is increased.

Measurements were then made relating intensity to beam potential at a constant current. An empirical equation predicting intensity as a function of the electron beam potential for x-ray tubes was determined by Green and Cosslett (Ref 6:1). The equation is

$$I = K \left( \frac{V}{E_k} - 1 \right)^{1.67} \quad (17)$$

where  $K$  = a constant of proportionality

$V$  = electron beam potential

$E_k$  = K-shell binding energy

The intensities measured experimentally fit this equation very well. It was also noted that the relationship was valid

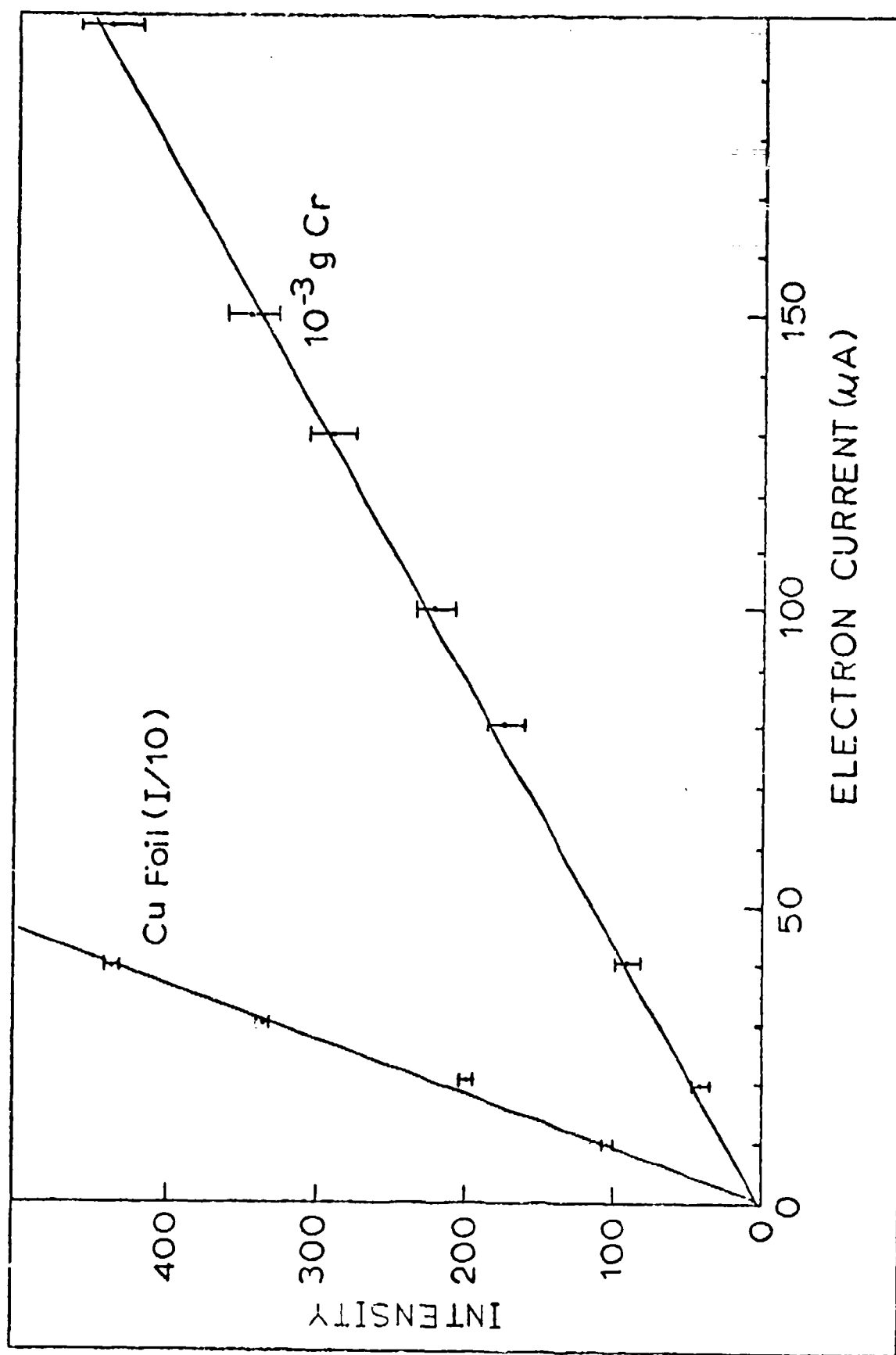


Fig. 15. Intensity as a Function of Electron Beam Current

for both the intensity of the radiation from the target measured directly or for the characteristic radiation emitted by a sample excited by the target radiation. The ratio  $I/K$  can be computed for a copper foil and plotted as a function of accelerating potential. This is shown in Fig. 16. If the ratio is plotted from experimental data obtained by exciting a copper sample with x rays from a rhodium target, the result is the same and the curves coincide. Within the limits of random counting error, the values of  $K$  are the same for all data points assuming a constant geometry and using the  $E_k$  of the radiation whose intensity is measured. The  $I/K$  ratios of several other elements are also plotted in Fig. 16 and show that the rate of increase in intensity becomes greater as atomic number decreases. This occurs because the efficiency of production of x rays by electrons becomes greater as the difference between  $E_k$  and electron energy increases.

From the preceding discussion, it can be seen that count rate increases with both beam current and voltage. For large solid samples, an adequate count rate can be achieved at low electron currents and energies and has the advantage of decreasing the power input to the target. On the other hand, the peak to background ratio was found to increase with beam potential.

For trace analysis, both count rate and the peak to background ratio are of primary importance. The minimum detectable concentration of an element occurs when the observed peak rises above the local background by at least twice the

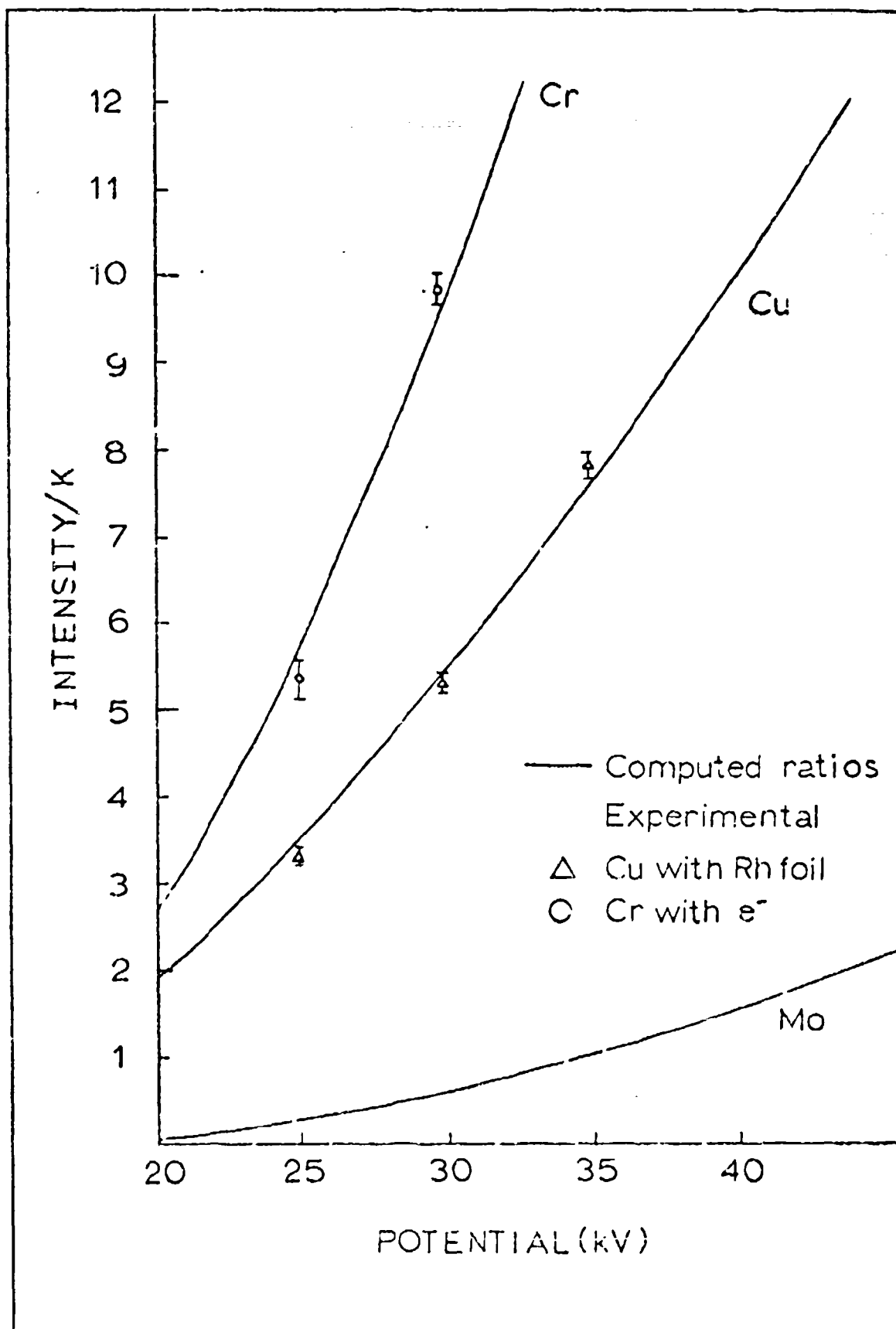


Fig. 16. Intensity as a Function of Electron Beam Potential

standard deviation of the background (Ref 24:16). This relation is written

$$C_{Min} = \frac{2\sqrt{B}}{I} C_{Std} \quad (18)$$

where B = background counts

I = net peak count above the background

C<sub>Std</sub> = concentration of the element analyzed

The minimum detectable concentration increases as the square root of the count rate, and the highest count rate is achieved at the highest beam current and accelerating potential available.

The diameter of the electron beam and the distance between the sample and the target foil also affected the x-ray intensity. The intensity of characteristic x rays emitted from a sample increased as the target was moved closer to the sample. At distances closer than 4 cm, little change in intensity was observed and this seemed to be the optimum. At this distance, with equal beam currents, a small concentrated beam seemed to produce a slightly higher count rate than a beam with a large diameter. Some data was taken to show the relationship of beam diameter to the other electron gun parameters. These data are presented in Table I. A large number of combinations are possible and these values do not represent any maximum or minimum sizes.

Table I  
Variation of Electron Beam Diameter  
With Other System Parameters

$I_F$ = Filament Current	$V_B$ = Beam Potential
$I_B$ = Beam Current	$V_F$ = Focusing Voltage
D = Beam Diameter	

---

$V_B$ (V)	$I_F$ (A)	D (in.)	$V_F$ (V)	$I_B$ ( A)
25	1.5	1/4	82	5
25	1.5	1/2	62	15
25	1.6	1/4	84	25
25	1.6	1/2	64	90
25	1.7	1/4	86	110
35	1.5	1/4	100	8
35	1.5	1/2	76	22
35	1.6	1/4	104	38
35	1.6	1/2	78	110
35	1.7	1/4	108	120

### Trace Element Analysis

The sensitivity of the system was determined by transmission foil excitation of reference solutions deposited on mylar. The lowest amount detectable was  $10^{-7}$  g and the K x rays of most elements that were excited with energies close to their absorption edge were detectable at that level. Chromium and iron were both detectable to  $10^{-7}$  g when excited with copper x rays, and rubidium was detected at that weight with molybdenum x rays. However, when molybdenum x rays were used to excite iron, only  $10^{-6}$  g of iron was detectable. The L x rays of lanthanum which had a fluorescent yield less than 0.1 were detected down to  $10^{-6}$  g with a copper foil. This indicates that the L x rays of heavier elements with higher

fluorescent yields should be detectable in the  $10^{-7}$  g range.

The intensities emitted from pure samples of iron, chromium, rubidium, and lanthanum were measured in concentrations from  $0.1 \mu\text{g}$  to  $0.01 \text{g}$ , and the results were plotted. Chromium and iron are shown in Fig. 17 and rubidium and lanthanum in Fig. 18. These curves were used as reference standards to determine the concentrations of these elements in substances of unknown composition. As long as matrix and self-absorption effects are absent, there is a direct proportionality between mass per unit area and intensity. The slopes of the curves in Fig. 17 and Fig. 18 are approximately unity and the straight portions represent linearity. When the specimens become thick and absorption occurs, this linearity breaks down. The concentrations at which this begins to occur is easily determined from the reference curves. The thickness at which absorption begins is a function of the sample element's x-ray energy, and of the amount of other elements present in the matrix. The chromium curve begins to break off at about  $400 \mu\text{g}$ , while rubidium with higher energy x rays that are less easily absorbed, exhibits linearity up to about  $1000 \mu\text{g}$ . These values compare favorably to those reported by other researchers (Ref 10,1). These limits can also be compared to those predicted by theory. Rhodes gives an equation for fluorescent intensity (Ref 26,268) which is

$$\frac{I_a}{K I_0} = \frac{\omega_a \tau_a}{\mu_1 + \mu_2} 1 - \exp - (\mu_1 + \mu_2)m \quad (19)$$

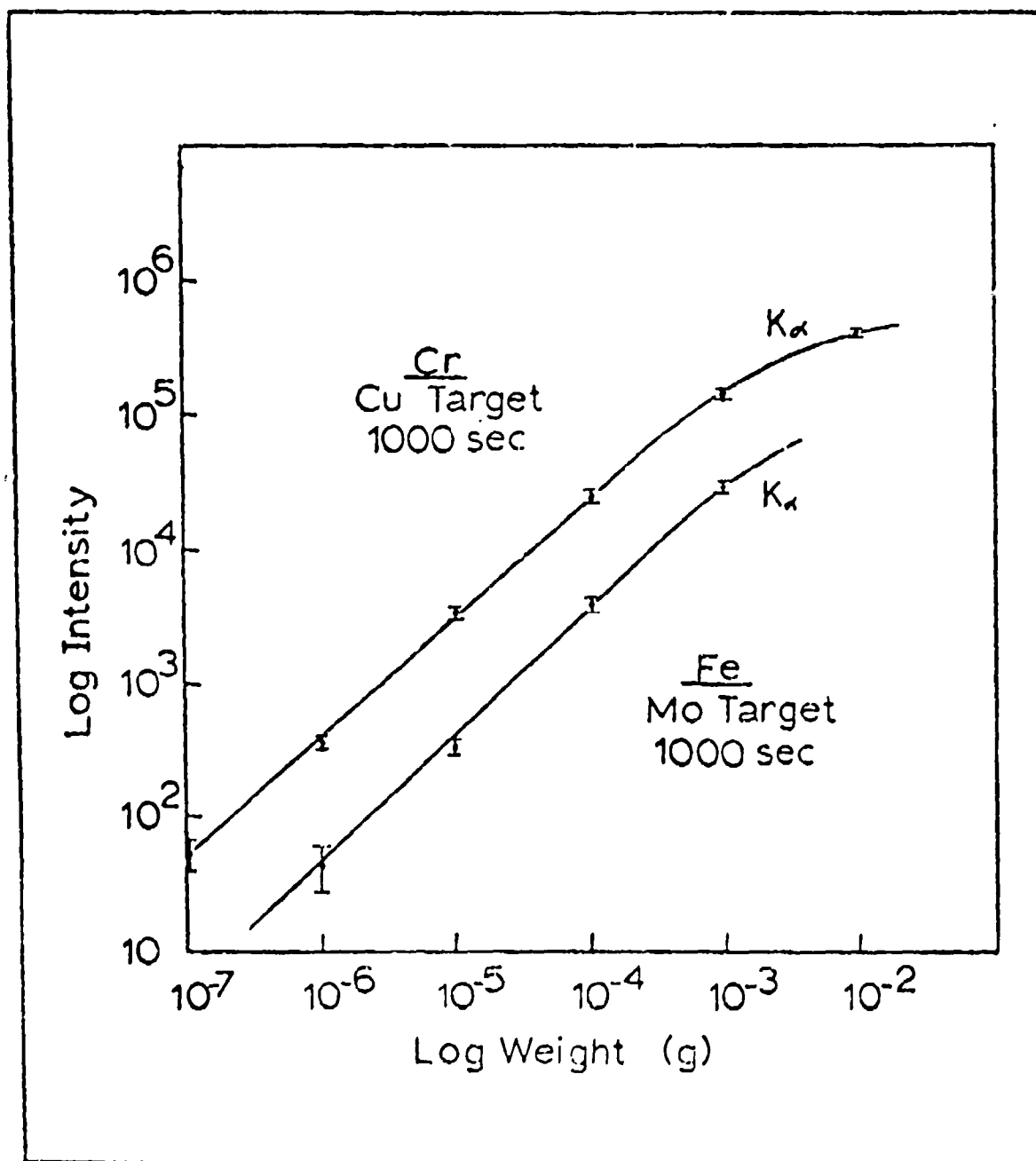


Fig. 17. Weight vs. Intensity for Cr and Fe



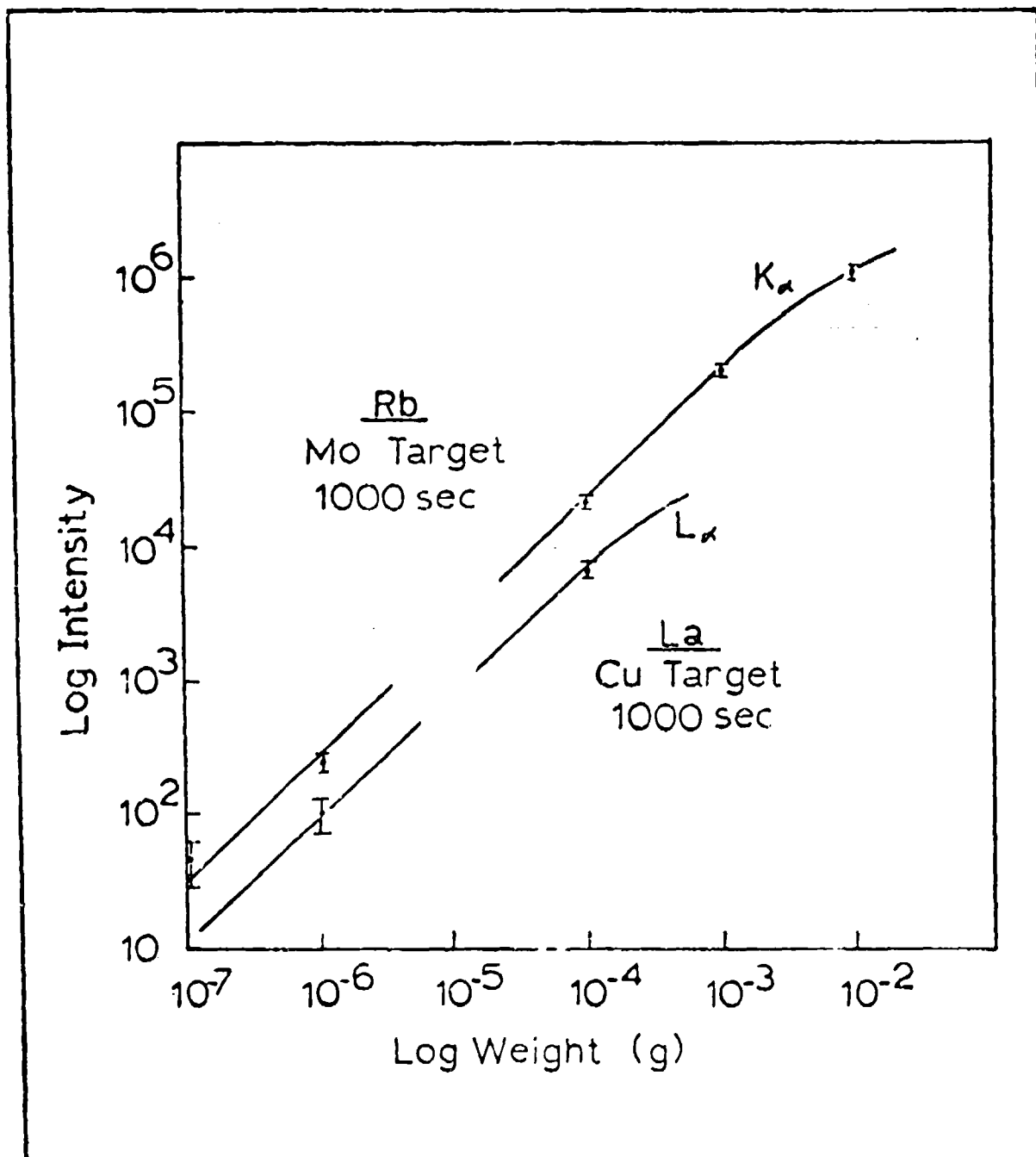


Fig. 18. Weight vs. Intensity for Rb and La

where  $K$  = constant combining geometrical factors and detector efficiency

$\omega_a$  = fluorescent yield of element 'a'

$\tau_a$  = photoelectric cross section for the incident radiation

$r_a$  = weight fraction of element 'a'

$m$  = mass per unit area

$\mu_1$  = attenuation coefficient at the incident energy

$\mu_2$  = attenuation coefficient at the fluorescent energy

A specimen is considered thin when

$$m(\mu_1 + \mu_2) \lesssim 0.1 \quad (20)$$

and Eq (19) then reduces to

$$\frac{I_a}{K I_o} = \omega_a \tau_a m_a \quad (21)$$

Setting Eq (20) equal to 0.1, solving for  $m_a$  and dividing by the area of the deposit yields the concentration at which the linearity breaks down for element a. The attenuation coefficients,  $\mu_1$  and  $\mu_2$ , depend on all the elements present in the deposit and are computed by

$$\mu_T = \sum_i \mu_i r_i \quad (22)$$

The value computed for rubidium using Eq (20) is  $1160 \mu g$  and compares well with the value determined from Fig. 18. For chromium, the computed value is  $397 \mu g$  which is also very close to the experimentally determined value. Since the

solutions used to make the samples are dissolved compounds, other elements are introduced which affect absorption in the specimen. Chromium is obtained from the salt,  $K_2CrO_4$ , and both oxygen and potassium will absorb chromium x rays. These other constituents cause the linearity to drop off earlier than it would if just the chromium were present. It is desirable to use compounds that have the elements of interest combined with others of low atomic number. However, in many cases, the most desirable compounds are insoluble and cannot be used.

Chromium was mixed individually with four other elements higher in atomic number and excited with molybdenum x rays to determine when enhancement of the chromium would occur. When  $10^{-4}$ g each of chromium and one of the other elements was mixed and excited, no enhancement was observed. At  $10^{-3}$ g, absorption of the chromium in the mixture was the same as that in a pure sample but no enhancement was apparent. However, when  $10^{-3}$ g of chromium was combined with  $10^{-2}$ g of several other elements of higher Z, the chromium was enhanced by as much as 30% when compared to the intensity from a pure sample.

The reference curves in Figs. 17 and 18 were used to analyze the constituents of some complex substances including atmospheric dust collected in an electrostatic precipitator and pulverized orchard leaves obtained from the National Bureau of Standards. The best technique for exciting specimens of unknown concentration was to make several runs using different transmission foils to examine different areas of

the spectrum. Elements that might not be detected with a single excitation energy can be found using this method. As an example of the importance of the energy of the exciting source, a 1.0 mg chromium sample excited with a silver target results in a peak of 4480 counts. The same sample excited with a copper target gives a peak with 141,127 counts, thirty times greater.

The N.B.S. orchard leaves was a reference standard and the amount of each constituent was given. It was not a particularly good sample for the dilution method because a minimum of 250 mg was required for guaranteed homogeneity, and only a few milligrams could be deposited in an area of 1.0 cm<sup>2</sup> on the mylar. However, some fairly good results were obtained using 3.3 mg  $\pm$  0.1 and 8.0 mg  $\pm$  0.1 samples. According to the N.B.S., the leaves contained 300  $\mu$ g/g  $\pm$  20 of iron. The 3.3 mg sample should then contain 0.9  $\mu$ g  $\pm$  0.07 of iron and the 8.0 mg sample should contain 2.4  $\mu$ g  $\pm$  0.16. Excitation of the 3.3 mg sample resulted in a peak with 648  $\pm$  25 counts. A 0.9  $\mu$ g pure iron sample was made from a reference solution and a series of runs resulted in an average of 627  $\pm$  4 counts in the peak. Neglecting matrix effects, the weight of the 8.0 mg sample can be computed by comparing its observed intensity, 1156  $\pm$  43 counts, to that of the 3.3 mg sample with the relation

$$\frac{I_U}{I_S} = \frac{W_U}{W_S} \quad (23)$$

where the U refers to the unknown and the S to the standard. The computed weight of  $2.57 \mu\text{g} \pm 0.24$  compares reasonably well to the value of  $2.4 \mu\text{g}$  determined from the N.B.S. data.

Atmospheric dust was also examined and provided an interesting specimen. It contained a large amount of iron whose weight was determined by reference to the calibration curve for iron in Fig. 18. The quantities of the other elements were determined from the iron intensity by correcting for the differences in fluorescent yield, cross section and detector efficiency with Eq (21). The incident intensity and geometrical factors were assumed to be constant. The spectrum of a 5.5 mg dust sample excited with a molybdenum target is shown in Fig. 19. The counting time was 1000 sec with a beam potential of 35 kV and a beam current of 200  $\mu\text{A}$ . Table II lists the elements identified in the sample with the concentrations of the larger constituents. When the same sample was excited with a copper target, the low atomic number elements were enhanced. For example, titanium had 1380 counts compared to about 30 with the molybdenum target. The presence of a cerium  $L_{\alpha}$  peak was also revealed by exciting the sample with copper x rays.

#### Matrix Effects

Four experiments were performed to investigate the concentrations of chromium, iron, and nickel in N.B.S. steel standards. The first two experiments were conducted with transmission targets as the exciting source in an attempt to selectively excite the elements in the steel and determine

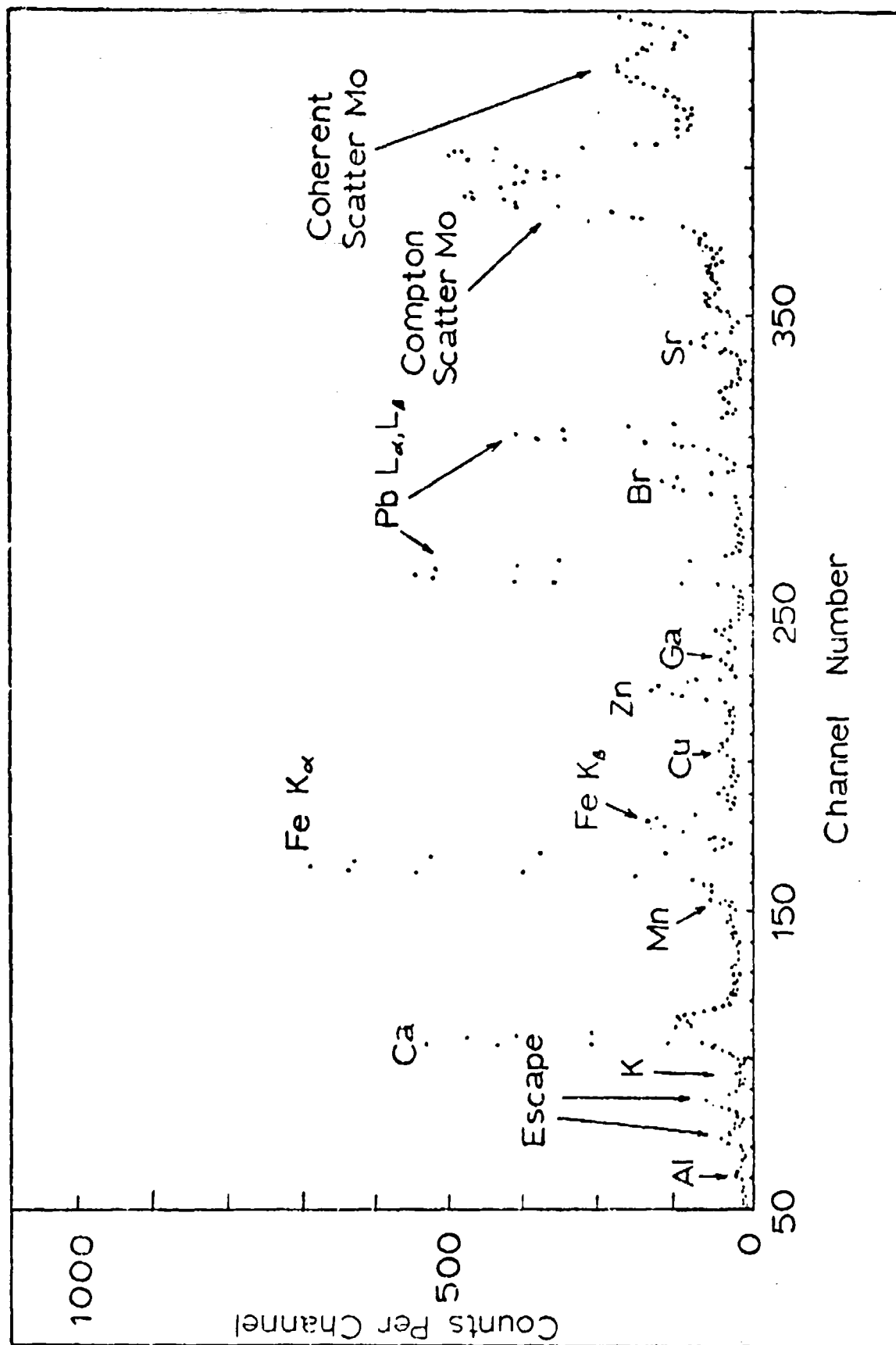


Fig. 19. Spectrum from Atmospheric Dust Excited with a Mo Target

Table II  
Contaminants in Atmospheric Dust (5.5 mg)

Time = 1000 sec		$I_B = 200 \mu A$	$V_B = 35 \text{ kV}$
Target = Molybdenum			
Element	Counts in Peak	Estimated Weight ( $\mu g$ )	% of Sample
Sulfur	25	—	—
Potassium	33	—	—
Calcium	2290	$297 \pm 9$	5.40
Titanium	30	—	—
Manganese	45	—	—
Iron	3442	$94 \pm 3$	1.70
Copper	27	—	—
Zinc	625	$8.3 \pm 0.5$	0.15
Gallium	79	$0.89 \pm 0.2$	0.016
Bromine	570	$4.74 \pm 0.28$	0.86
Strontium	349	$2.1 \pm 0.18$	0.38
Zirconium	65	—	—
Lead	1960	$13 \pm 0.43$	0.24

correction factors for enhancement and absorption interactions. The first attempt was made using the radiation transmitted through a thick iron foil to excite the sample directly. Since iron x rays will not excite iron and nickel, only the chromium should have been excited. However, a large amount of bremsstrahlung high enough in energy to excite iron and nickel was also transmitted, and the chromium intensity in the steel was enhanced when compared to a pure sample of chromium excited under the same conditions. The use of a secondary target geometry was also tried in an attempt to

reduce the bremsstrahlung spectrum, and the results were a little better, but bremsstrahlung transmitted through the molybdenum foil and scattered from the iron secondary still produced enough iron x rays in the steel to enhance the chromium intensity. The results of these two experiments compared to the actual chromium concentrations in the steel alloys are shown in Table III.

Table III  
Enhancement of Chromium in Steel From an Iron Target  
Used as Both a Primary and Secondary Exciting Source

Alloy	Chemical Concentration of Cr (%)	Primary (%) <sup>a</sup>	Secondary (%) <sup>a</sup>
845	13.31	20.85 $\pm$ 0.59	19.02 $\pm$ 1.1
846	18.35	28.90 $\pm$ 0.73	26.90 $\pm$ 2.0
848	9.09	15.67 $\pm$ 0.50	12.23 $\pm$ 0.83
850	2.99	5.96 $\pm$ 0.30	4.19 $\pm$ 0.46

<sup>a</sup>Determined by comparison to pure Cr excited under the same conditions.

The final two experiments were conducted with direct electron excitation. Selective excitation of the elements in the steel standards was attempted first. With the electron beam energy just above the absorption edge of chromium and below that of iron, it was possible to excite only the chromium. But the efficiency of production of x rays at this energy is so low that the peak was barely detectable above the continuous background and no reliable data could be obtained.

The excitation of the samples with a higher energy beam and as small a beam diameter as possible gave better results.



The reduction in the size of the beam reduces the total amount of bremsstrahlung, and the peak to background ratio is increased because the dead time is reduced. It was found throughout the study that dead times in excess of about 10% resulted in lower peak to background ratios. Large amounts of low energy bremsstrahlung also degrade the resolution in spite of the Scotch Tape absorber, and the use of the small beam is required to keep the current low and reduce the total continuous radiation emitted. The most important result from the use of a focused beam in this experiment is the reduction in matrix effects by reducing the volume of the excited material.

The use of beam potentials above 20 kV allowed the samples to be excited much more efficiently and had the most significant effect on increasing the peak to background ratio. Beam potentials higher than 25 kV should be avoided, however, because the more energetic electrons penetrate more deeply into the sample. Because of the short range of the electrons in the samples, most of the x-ray production occurred close to the surface and very little enhancement or absorption was observed. The four alloys examined were compared with a pure chromium sample excited under the same conditions and the agreement with the actual chemical composition was very good. The results of these runs are listed in Table IV.

If no matrix effects are present and no difference in detection efficiency or x-ray production efficiency exists, the relative intensities of the elements in a substance should be equal to their weight fractions. Since the detector

efficiency for iron, nickel, and chromium is 100% for the germanium detector used in this work, correction of the observed intensities for x-ray production efficiency by electrons should yield the actual intensities assuming no matrix effects.

Determination of these production efficiencies proved to be a problem. The efficiency is a function of the beam voltage, the take-off angle (angle between the emitted x rays and the sample surface) and the angle of the electron beam to the sample surface. The angle of the sample to the electron beam in this experiment was  $45^\circ$  and no data was available for these geometrical conditions.

An alternative method was to use one of the samples as a standard and compute the efficiency ratios. The efficiency is expressed in the literature as photons per electron per steradian and accounts for both atomic weight and fluorescent yield. The efficiency of production is related to peak intensity by

$$\epsilon_1 N_1 \propto C_1 \quad (24)$$

where

$\epsilon_1$  = efficiency of production of x rays by electrons

$N_1$  = number of atoms/cm<sup>3</sup>

$C_1$  = net counts in the photo peak

Two elements in a sample can then be related by

$$\frac{N_1}{N_2} = \frac{C_1 \epsilon_2}{C_2 \epsilon_1} \quad (25)$$

The weight fraction of an element in the sample is proportional to the number of atoms and the density by the relation

$$W_1 \propto \frac{N_1}{\rho_1} \quad (26)$$

where

$W_1$  = weight fraction of an element in the sample

$\rho_1$  = density

The ratio of the weight fraction of two elements in the sample can then be determined by

$$\frac{W_1}{W_2} = \frac{\rho_2 \epsilon_2 C_1}{\rho_1 \epsilon_1 C_2} \quad (27)$$

The efficiency ratios determined for the reference sample were used to correct the intensities of the other samples. The results were reasonably close considering the magnitude of the random counting error at these intensities. The results are presented in Table IV with the chromium concentrations determined by comparison to a pure sample. Since the three elements analyzed accounted for a little less than 100% of the sample, a correction was made in the total intensities for this difference.

Table IV  
Composition of Steel Estimated by  
Direct Electron Excitation

Alloy	Element	Chemical Wt. (%)	Corrected for Production Efficiency (%)	Compared To Pure Element (%)
845	Cr	13.31	$14.16 \pm 0.26$	$14.8 \pm 0.25$
	Fe	83.20	$82.40 \pm 1.8$	
	Ni	0.28	$0.21 \pm 0.03$	
846	Cr	18.35	Reference	$18.12 \pm 0.28$
	Fe	68.80		
	Ni	9.11		
848	Cr	9.09	$9.16 \pm 0.26$	—
	Fe	85.30	$85.46 \pm 2.7$	
	Ni	0.52	$0.26 \pm 0.05$	
850	Cr	2.99	$2.10 \pm 0.06$	$3.20 \pm 0.11$
	Fe	70.80	$73.00 \pm 2.8$	
	Ni	24.80	$23.90 \pm 1.1$	

VI. CONCLUSIONS AND RECOMMENDATIONS

The goal of this study was to construct and investigate the capabilities of a system for energy dispersive x-ray analysis which uses an electron gun as an exciting source. The capabilities of the system for both qualitative and quantitative analysis were very good and can be substantially improved with the modifications recommended in this section. With 1000 sec counting times, weights in the  $10^{-7}$  g range were detected. However, this value is limited by the geometry imposed by the size of the chamber. The detector could not be placed any closer to the sample than 9.5 in., and the small solid angles limit the amount of sample radiation seen by the detector. With the detector positioned a few centimeters from the sample, the limit of detection should be at least an order of magnitude lower.

In a study done currently with this project, the use of radioisotope excitation produced minimum detectable concentrations of  $10^{-6}$  g, but required long counting times even with the source, sample, and detector only a few centimeters apart. For example, when the silver x rays from a 3 mCi  $\text{Cd}^{109}$  source were used to excite atmospheric dust, it took 16,000 sec to produce an iron peak with 4400 counts. With the electron gun and a molybdenum target to excite the same sample, 4400 counts were recorded in the iron peak in only 1000 sec.

Proton excitation done previously by this laboratory with a 2 MeV Van De Graaff accelerator produced detection of

concentrations in the nanogram range with counting times less than 2000 sec, and shows promise of even better sensitivity. A small amount of atmospheric dust deposited on a carbon foil and excited with 1.5 MeV protons produced an iron peak with 690,000 counts in 2000 sec of operation. The detector in this case was located approximately 2.5 in. from the sample. Fig. 5 shows that the intensity of x rays produced by 1.5 MeV protons should be about the same as the intensity produced by 25 keV electrons. Although the electrons were not used directly to excite the atmospheric samples, the large difference in count rate must be due primarily to the geometrical factors. Because of the extremely low level of bremsstrahlung, proton excitation is still preferred, but where accelerators are not available, the electron gun provides a good alternative.

Atmospheric dust was the only substance analyzed both qualitatively and quantitatively because of time limitations. Differences in composition were noted between different samples indicating that the elements were not homogeneously distributed and that the contaminants in the air probably vary over a period of several days. Other substances such as blood and pulverized concrete were examined briefly to determine the extent to which the dilution technique was applicable. Many substances do not dissolve in water and thin slurries made by mixing them with deionized water do not always adhere to mylar. A low atomic number vacuum grease was used to mount some samples without affecting the spectrum. All the

samples that were used had to be of the same area and general shape according to theory. It was determined by experiment that below concentrations of  $10^{-3}g$ , a 15 to 20% variation in area had no effect on the observed intensities.

Quantitative analysis with experimentally determined reference standards also has its drawbacks. It is a time-consuming process making standards for a large number of elements, and they must be checked and updated periodically to correct for variations in the detection equipment. Many techniques have been designed to compensate for matrix effects in various substances, but all suffer certain disadvantages and are limited to a narrow range of specimens to which they apply.

The use of direct electron excitation also looks promising for certain applications, but its range of capabilities was not fully explored and more investigation needs to be done in this area. The minimum beam diameter available with the system was never used experimentally, and its use would probably further reduce matrix effects in the samples.

It is recommended that more analysis be accomplished using the electron gun and that certain modifications be made to improve the sensitivity. Specifically, a new chamber should be designed to replace the Ortec chamber now in use. The detector to sample path needs to be reduced considerably, and provisions should be made for the use of multiple samples and targets similar to the carousel sample holder used in this system. The position of the electron gun could be made variable to take better advantage of its focusing

characteristics, and to allow longer counting times some method of cooling the target should be devised. A design proposal for an improved sample chamber is presented in Appendix C.

The errors introduced into the data were larger in many cases than would be expected from counting statistics. This probably resulted from problems associated with the detector and analyzer which were present throughout the experimental period. Many runs were taken and some data discarded to obtain consistent results but the deviations in some values are still rather large. The statistical methods used in reduction of the data is included in Appendix B.

In summary, the versatility of the electron gun as an excitation source and the higher level of photon flux it produces gives it an advantage over radioisotope excitation even using very active sources. Compared to proton excitation, the main advantage of the electron gun is its lower cost and greater availability.



Appendix A

List of Equipment

1. Keithly Instruments Model 153 Microvolt-Ammeter
2. Spellman High Voltage Power Supply  
60 kV at 1 mA
3. Norton Vacuum Equipment NRC 831 Ionization Gauge Control
4. Consolidated Vacuum Corp. Ionization Gauge Tube
5. Consolidated Vacuum Corp. Six-inch Oil Diffusion Pump
6. Nuclear Data Model 2200 Modular Multichannel Analyzer  
with the following modules:
  - A. Memory
  - B. Master Control
  - C. Read-in/Out Display
  - D. Dual Parameter Input/Display
  - E. Analog to Digital Converter  
Conversion Gain: 2048  
Input: D.C.  
BLR: Out
  - F. Teletype Drive
  - G. Magnetic Tape Read
  - H. Magnetic Tape Control/Write
7. Peripheral Equipment Corp. Magnetic Tape Transport
8. Hewlett Packard Oscilloscope
9. Ortec Model 452 Spectroscopy Amplifier  
Coarse Gain: 100  
Shape Time: 3  $\mu$  sec

Output Range: + 10v

Output: Unipolar

Delay: Out

BLR: Out

10. Technical Measurements Corp. Teletype

11. Hewlett-Packard Harrison 6516A D.C. Power Supply

Bias: -660v

12. General Electric Series 411 High Purity Germanium Photon Spectrometer

## Appendix B

Statistical Treatment

The data used to plot the reference curves was obtained by taking a number of runs under the exact same conditions and averaging the net counts to obtain the arithmetic mean. The count rate fluctuated excessively between some runs because of suspected problems in the detector or analyzer and the differences in gross counts were large. However, the same variations were reflected in the background and the net counts were often very close. Therefore out of necessity, the statistical treatment was based on the net counts. The total variation was computed from

$$\sigma_T = \left[ \frac{\bar{n} - n_1}{N-1} \right]^{\frac{1}{2}} \quad (28)$$

where  $N$  = number of readings

$\bar{n}$  = arithmetic mean

$n_1$  = net counts for each run

The standard deviation of the arithmetic mean value is then given by

$$\sigma_{\bar{n}} = \frac{\sigma_T}{\sqrt{N}} \quad (29)$$

The total variation includes the instrument operation error, counting error, sample variation error, and the instrument variation error (Ref 4:2). The sample variation and

instrument operation errors were assumed negligible compared to the instrument variation and counting errors. The magnitude of the instrument error can be estimated from the relationship

$$\sigma_T = [\sigma_C^2 + \sigma_I^2]^{\frac{1}{2}} \quad (30)$$

where  $\sigma_C$  = counting error  
 $\sigma_I$  = instrument variation

The net peak areas for a typical series of chromium runs is shown in Table V.

Table V  
 Net Peak Areas From the Excitation of  $10^{-5}$  g of Chromium

N	Net Peak Counts	$(\bar{n} - n_i)^2$
1	2492	400
2	2335	18769
3	2590	13924
$\bar{n}$	2472	33092

Using the values from Table V and Eq (25) the total variation,  $\sigma_T$ , is computed as 128.6. The instrument variation can then be calculated:

$$\sigma_I = [\sigma_T^2 - \sigma_C^2]^{\frac{1}{2}} = (16538 - 2472)^{\frac{1}{2}} = 118.5 \quad (31)$$

This result indicates that the instrument variation is the largest error associated with these runs.

The data obtained from direct electron excitation was generally based on one observation and the variation of the measurements were due to random counting error alone. The standard deviation of a measurement is just the square root of that measurement. With spectral peaks, the background as well as the characteristic peak itself must be statistically considered. The standard deviation is calculated from

$$\sigma = (C_g + C_b)^{\frac{1}{2}} \quad (32)$$

where  $C_g$  = gross counts under the peak  
 $C_b$  = background counts

Some of the computations involved the multiplication or division of quantities that had errors associated with their values, and these errors had to be propagated to determine the total error. If A and B are multiplied or divided to form C, the total error is determined by

$$\frac{\sigma_C}{C} = \left[ \left( \frac{\sigma_A}{A} \right)^2 + \left( \frac{\sigma_B}{B} \right)^2 \right]^{\frac{1}{2}} \quad (33)$$

## Appendix C

Proposed Chamber

The scattering chamber illustrated in Fig. 20 is proposed as a replacement for the Ortec chamber used in this study. The new chamber is designed so that the detector is much closer to the sample to improve the sensitivity. The carousels shown in the diagram rotate and can hold up to six samples or target foils. Target cooling is accomplished by extending the target carousel support through the chamber bottom and into a liquid nitrogen reservoir. The beam current is also measured from this support and the carousel control rod must be insulated from the chamber.

The construction of the cylindrical chamber should be primarily of high purity aluminum with glass or plexiglass windows in the top for visual positioning of the targets and samples. These windows can then be covered with lead shields while the gun is operating. Thin lead sheets may be required also on the inside shields to prevent penetration of scattered high energy bremsstrahlung which may enter the detector. Experimentation with shielding in the sample chamber may be necessary to determine the optimum arrangement.

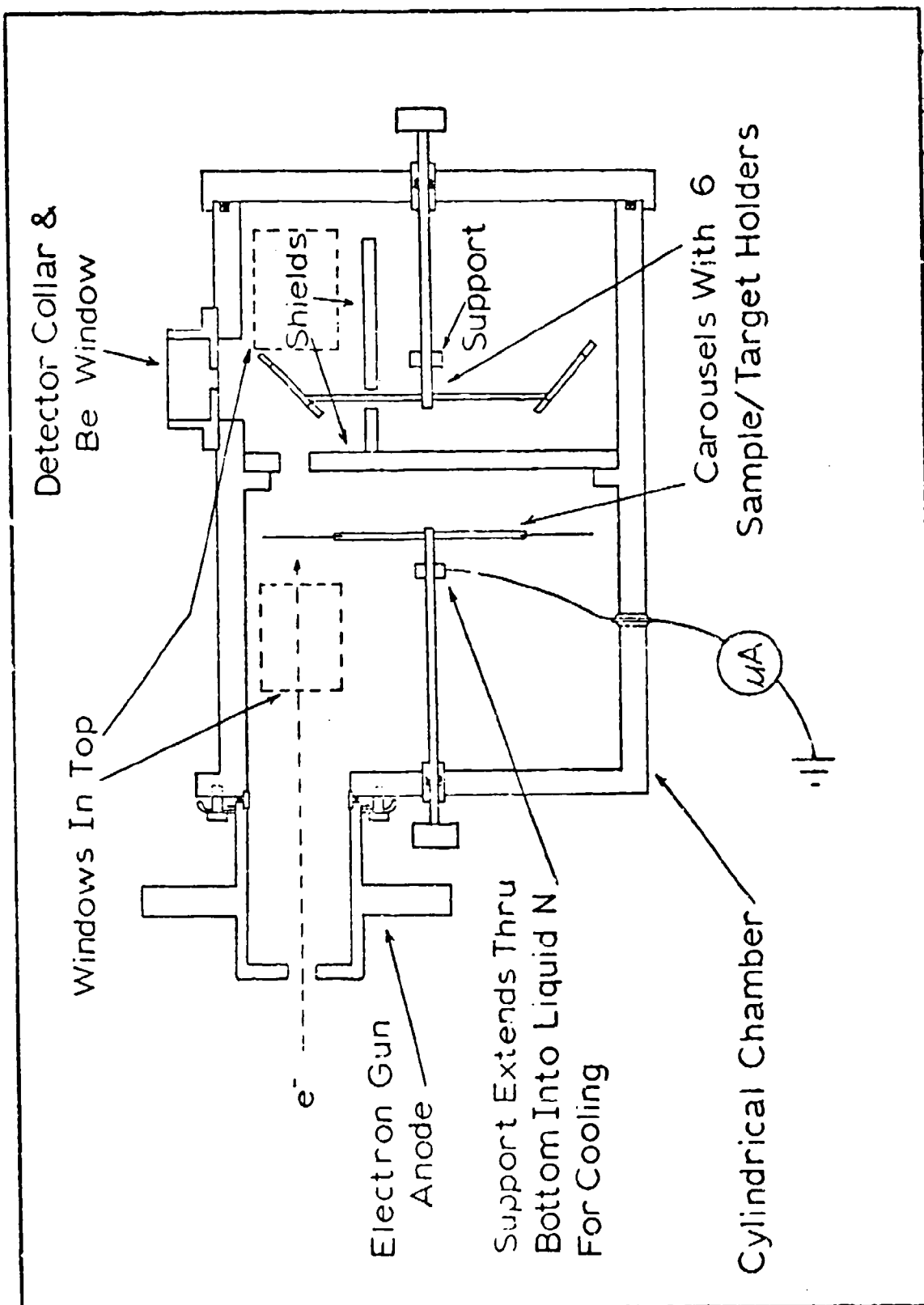


Fig. 20. Proposed Sample Chamber

BIBLIOGRAPHY

1. Banerjee, B. R. and W. D. Bingle. "Industrial Applications of Microprobe Analysis" in Developments in Applied Spectroscopy, edited by J. E. Forrette. New York: Plenum Press, 1964.
2. Birks, L. S. X-ray Spectrochemical Analysis. New York: Interscience Publishers, 1969.
3. Blackwelder, L. S. Methods of Photopeak Analysis for Gamma-Ray Spectra. Unpublished thesis. Wright-Patterson Air Force Base, Ohio: Air Force Institute of Technology, March, 1971.
4. Braucks, F. W. "Untersuchungen an der Fernfokuskathode Nach Steigerwald." OPTIK, 15: 212-260 (1957).
5. Brown, D. B. and R. E. Ogilvie. "Efficiency of Production of Characteristic X-Radiation from Pure Elements Bombarded by Electrons." Journal of Applied Physics, 35: 309-314 (February 1964).
6. Croke, J. F. and W. R. Kiley. "Specimen-Preparation Techniques" in Handbook of X-rays, edited by Emmett F. Kaelble. New York: McGraw-Hill Book Co., 1967.
7. Goulding, F. S. and J. M. Jaklevic. Trace Element Analysis by X-ray Fluorescence. UCRL-20625.
8. Green, M. and V. E. Cosslett. "The Efficiency of Production of Characteristic X-Radiation in Thin Targets of a Pure Element." Proceedings of the Physical Society, 78: 1206-1214, (1961).
9. Gunn, E. L. "Quantitative Techniques" in Handbook of X-rays, edited by Emmett F. Kaelble. New York: McGraw-Hill Book Co., 1967.
10. Gunn, E. L. "X-ray Fluorescent Intensity of Elements Evaporated from Solution onto Thin Film." Analytical Chemistry, 33: 921-927 (June 1961).
11. Harvey, B. G. Introduction to Nuclear Physics and Chemistry. Englewood Cliffs, New Jersey: Prentice Hall Inc., 1969.
12. Hockemoier, J. M. Elemental and Trace Analysis by Energy Dispersive X-ray Spectrometry. Unpublished thesis. Wright-Patterson Air Force Base, Ohio: Air Force Institute of Technology, March, 1972.



13. Holman, J. P. Heat Transfer. New York: McGraw-Hill Book Co., 1968.
14. Hurst, G. S. and J. E. Turner. Elementary Radiation Physics. New York: John Wiley and Son, Inc., 1970.
15. Jaklevic, J. M., et al. Small X-ray Tubes for Energy Dispersive Analysis Using Semiconductor Spectrometers. LBL-10.
16. Johansson, T. B., et al. "X-ray Analysis: Elemental Trace Analysis at the  $10^{-12}$  g Level." Nuclear Instruments and Methods, 84: 141-143 (1970).
17. Lange, N. A. Handbook of Chemistry. New York: McGraw-Hill, 1952.
18. Lederer, C. M., et al. Table of Isotopes. New York: John Wiley and Sons, Inc., 1968.
19. Lepage, J. and R. Jackson. Fluorescent Yield Measurements. DASA 2601.
20. Liebhafsky, H. A., et al. X-ray Absorption and Emission in Analytical Chemistry. New York: John Wiley and Sons, Inc., 1960.
21. Loomis, T. C. and S. M. Vincent. "Trace and Micro-analysis" in Handbook of X-rays, edited by Emmett F. Kaelble. New York: McGraw-Hill Book Co., 1967.
22. McCrary, J. H. and T. Van Vorous. The Use of Field Emission Tubes in X-ray Analysis. Vacuum Technology Associates, Broomfield, Colorado.
23. Modern X-ray Analysis. Nuclear Diodes, Inc. Prairie View, Illinois.
24. Modern X-ray Analysis II. EDAX International, Inc. Prairie View, Illinois.
25. Price, W. J. Nuclear Radiation Detection. New York: McGraw-Hill Book Co., 1958.
26. Rhodes, J. R. "Design and Application of X-ray Emission Analyzers Using Radioisotope X-ray or Gamma Ray Sources." Energy Dispersive X-ray Analysis: X-ray and Electron Probe Analysis. American Society for Testing and Materials, ASTM STP 485, 1971.
27. Russ, J. C. "Light Element Analysis Using Semiconductor X-ray Energy Spectrometer with Electron Excitation." Energy Dispersive X-ray Analysis: X-ray and Electron Probe Analysis. American Society for Testing and Materials, ASTM STP 485, 1971.

28. Sandborg, A. O. "Energy Dispersion X-ray Analysis with Electron and Isotope Excitation." Energy Dispersive X-ray Analysis: X-ray and Electron Probe Analysis. American Society for Testing and Materials, ASTM STP 485, 1971.
29. Storm, E. and H. I. Israel. "Photon Cross Sections from 1 keV to 100 MeV for Elements Z=1 to Z=100." Nuclear Data Tables, 7: 565-681 (June 1970).
30. Walter, F. J. "Characterization of Semiconductor X-ray Energy Spectrometers." Energy Dispersive X-ray Analysis: X-ray and Electron Probe Analysis. American Society for Testing and Materials, ASTM STP 485, 1971.
31. Wehr, M. R. and J. A. Richards. Physics of the Atom. London: Addison-Wesley Publishing Co., 1967.

VITA

William Charles Nielsen, Jr. was born March 10, 1943 in Columbus, Mississippi. He graduated from Chaminade High School in Dayton, Ohio in 1961 and then attended the United States Air Force Academy, graduating in 1965 with a Bachelor of Science degree. He entered pilot training at Laredo AFB, Texas receiving his wings in 1966 and then moving on to Davis-Monthan AFB, Arizona for combat crew training in the F-4 aircraft. Nine months of combat flying at Ubon Air Base in Thailand ended with reassignment to Laredo as a T-38 Flight Instructor. In 1971 he was selected to attend the Air Force Institute of Technology as a Master of Science degree candidate in Engineering Physics.

Permanent address: 11201 Loch Lomond Road  
Los Alamitos, California

This thesis was typed by Mrs. Eleanor Schwab.